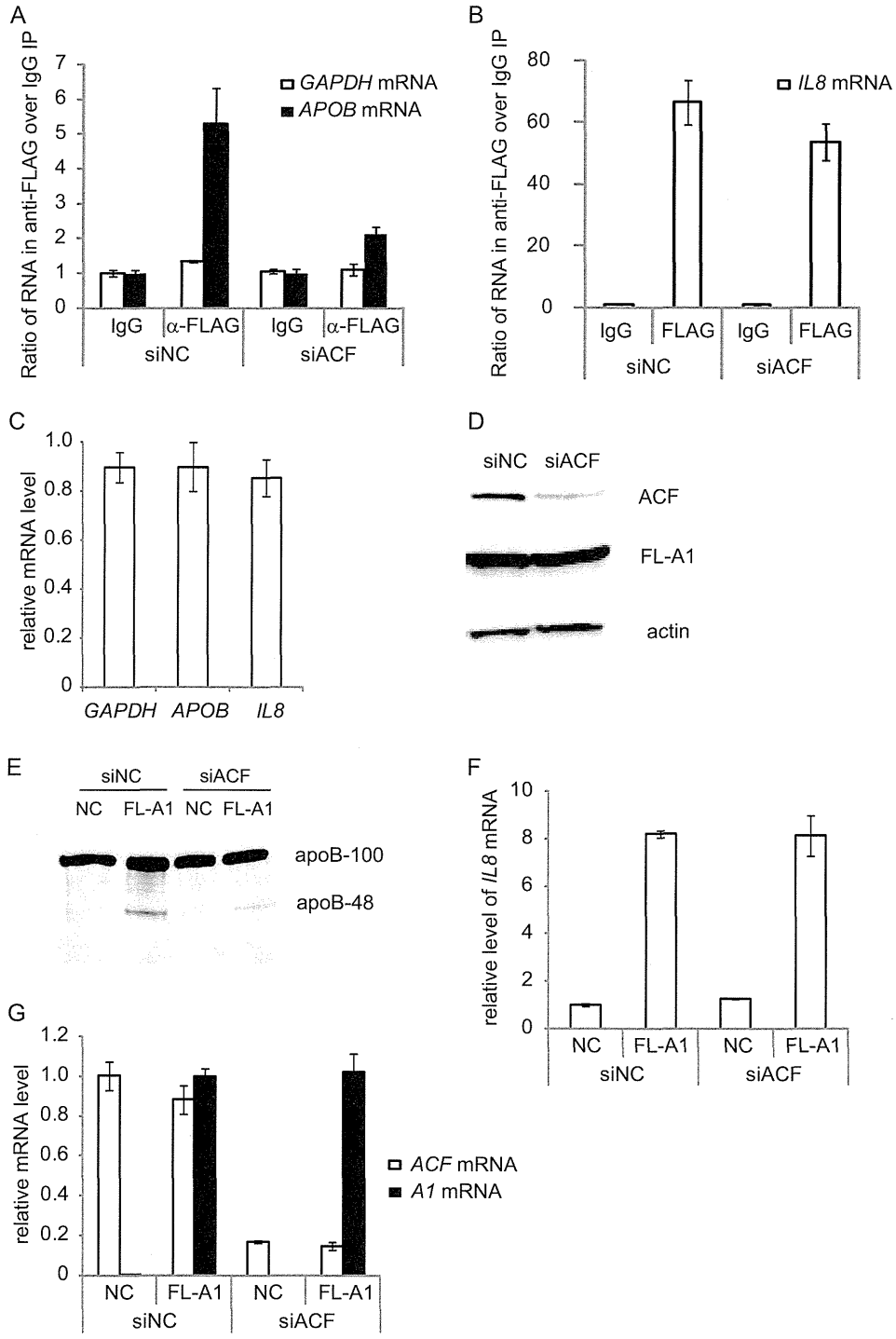

FIGURE 4. **Knockdown of ACF attenuates APOBEC1-mediated *APOB* editing but does not affect the APOBEC1-mediated increase in *IL8* mRNA expression.** *A*, the effect of knockdown of ACF on binding of APOBEC1 to *APOB* mRNA. HuH7.5 cells were reverse-transfected with a control (*si-NC*) or ACF-specific (*si-ACF*) siRNA (30 nM) and then transfected with the FL-A1 plasmid 16 h later. The cells were harvested 48 h after transfection and lysed in RIPA buffer. Each lysate was divided into two fractions, one of which was reacted with control IgG and the other with an anti-FLAG antibody. Each immunoprecipitate was subjected to RNA extraction and RT-qPCR analyses of *APOB* and *GAPDH* (control) mRNA levels. For each mRNA, the data were normalized to the level of RNA immunoprecipitated with control IgG. Data are represented as the mean ± S.D. (*error bars*) of $n = 3$ replicate samples. *B*, the effect of knockdown of ACF on binding of APOBEC1 to *IL8* mRNA. The cDNA samples prepared as described in *A* were subjected to RT-qPCR analyses to detect *IL8* mRNA expression. The data were normalized to the level of RNA immunoprecipitated with control IgG. Data are represented as the mean ± S.D. of $n = 3$ replicate samples. *C*, RT-qPCR analyses of *GAPDH*, *APOB*, and *IL8* mRNA levels in the cells described in *A*. The relative mRNA levels in cells treated with si-ACF compared with those treated with si-NC are shown. Data are represented as the mean ± S.D. of $n = 3$ replicate samples. *D*, immunoblot analyses of ACF, FL-A1, and actin (control) in lysates prepared from the cells described in *A*. *E*, the effect of knockdown of ACF on *APOB* editing by APOBEC1. HuH7.5 cells were reverse-transfected with si-NC or si-ACF (30 nM) and then transfected with empty plasmid (pCAG-FLAG; *NC*) or the FL-A1 plasmid 16 h later. The culture medium was harvested 48 h after transfection and used for immunoblot analyses of apoB-100 and apoB-48. *F*, the effect of knockdown of ACF on the APOBEC1-mediated increase in *IL8* mRNA expression. The HuH7.5 cells described in *E* were harvested 48 h after transfection and subjected to RNA extraction and RT-qPCR analyses. The *IL8* mRNA levels were normalized to those of *GAPDH*. Data are represented as the mean ± S.D. of $n = 3$ replicate samples. *G*, RT-qPCR analyses of *ACF* and *A1* mRNA levels in the cells used in *E*. The expression level of each mRNA was normalized to that of *GAPDH*. Data are represented as the mean ± S.D. of $n = 3$ replicate samples.

TABLE 1

Proteins identified in a yeast two-hybrid analysis in which APOBEC1 was used as the bait

For hnRNPQ and hnRNPR, two isoforms were identified as candidate binding partners of APOBEC1.

Number	Protein	Isoform
1	Heterogeneous nuclear ribonucleoprotein K	Isoform a
2	Heterogeneous nuclear ribonucleoprotein Q	Isoform 2
	Heterogeneous nuclear ribonucleoprotein Q	Isoform 4
3	Heterogeneous nuclear ribonucleoprotien R	Isoform 3
	Heterogeneous nuclear ribonucleoprotien R	Isoform 4
4	Heterogeneous nuclear ribonucleoprotein U-like protein 2	
5	RNA-binding protein Raly	Isoform 1
6	RNA-binding protein Fox-1 homolog 3	
7	G protein-coupled receptor-associated sorting protein 1	
8	KH domain-containing, RNA binding, signal transduction-associated protein 1	
9	Extracellular matrix protein 1	Isoform 2
10	Amino-terminal enhancer of split	Isoform a
11	Thioredoxin domain-containing protein 11	

(Fig. 4*D*). Knockdown of ACF attenuated FL-A1-mediated apoB-48 production but did not affect the FL-A1-mediated increase in *IL8* mRNA expression (Fig. 4, *E* and *F*). In this experiment, knockdown of ACF did not affect the *FL-A1* mRNA level, and overexpression of FL-A1 did not affect *ACF* mRNA expression (Fig. 4*G*). These results suggest that, unlike *APOB* editing, the APOBEC1-mediated increase in *IL8* mRNA expression does not require ACF.

Next, a yeast two-hybrid analysis was performed to identify possible other complementing proteins that promote binding of APOBEC1 to *IL8* mRNA. In this experiment, a human brain cDNA library was used as prey, and APOBEC1 was used as bait. Of the 21 colonies isolated, five encoded hnRNPR isoform 4, three encoded hnRNPQ isoform 2, three encoded KH domain-containing RNA-binding signal transduction-associated protein 1, and the remainder encoded 10 different proteins. Eleven different proteins were identified as potential binding partners of APOBEC1 (Table 1). Two isoforms of hnRNPQ (hnRNPQ2 and -4) and two isoforms of hnRNPR (hnRNPR3 and -4), were included in the list of candidates. Another candidate, RNA-binding protein Fox-1 homolog 3, was not expressed in HuH7.5 cells (data not shown).

Knockdown of hnRNPQ Reduces Binding of APOBEC1 to IL8 mRNA in HuH7.5 Cells—To determine whether any of the 11 candidate binding partners of APOBEC1 enhance or facilitate the interaction between APOBEC1 and *IL8* mRNA, we examined the effect of siRNA-mediated knockdown of each protein on co-IP of FL-A1 and *IL8* mRNA from HuH7.5 cell extracts. For two candidates (hnRNPQ and hnRNPR), siRNAs that were complementary to both isoforms identified as candidate binding partners of APOBEC1 were used. The siRNA targeting hnRNPQ (si-hnRNPQ) was the only siRNA that affected co-IP of FL-A1 and *IL8* mRNA (Fig. 5*A*) (data not shown). Transfection of HuH7.5 cells with si-hnRNPQ caused a 70% decrease in *hnRNPQ* mRNA levels (Fig. 5*B*) but did not affect FL-A1 protein expression (Fig. 5*C*). Furthermore, knockdown of hnRNPQ also reduced *IL8* mRNA levels slightly (Fig. 5*D*). These findings indicate that hnRNPQ contributes to the association between *IL8* mRNA and ectopically expressed FL-A1 in HuH7.5 cells.

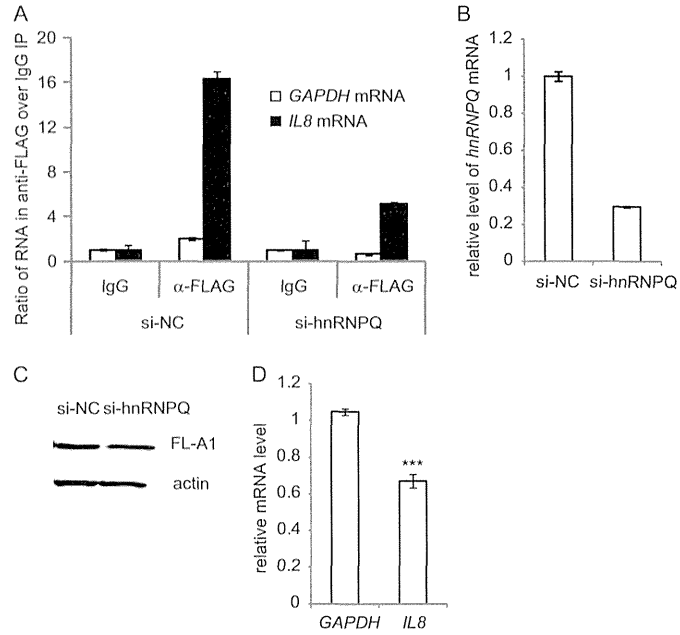

FIGURE 5. **Knockdown of hnRNPQ attenuates binding of APOBEC1 to *IL8* mRNA in HuH7.5 cells.** *A*, the decrease in binding of APOBEC1 to *IL8* mRNA following knockdown of hnRNPQ. HuH7.5 cells were reverse-transfected with a control (*si-NC*) or hnRNPQ-specific (*si-hnRNPQ*) siRNA (30 nM) and then transfected with the FL-A1 plasmid 16 h later. The cells were harvested 48 h after transfection and lysed in RIPA buffer. Each lysate was divided into two fractions, one of which was reacted with control IgG and the other with an anti-FLAG antibody. Each immunoprecipitate was subjected to RNA extraction and RT-qPCR. For each mRNA, the amount in the anti-FLAG immunoprecipitate was normalized to that in the IgG immunoprecipitate. Data are represented as the mean ± S.D. (*error bars*) of $n = 3$ replicate samples. *B*, RT-qPCR analyses of the effect of transfection of HuH7.5 cells with a hnRNPQ-specific siRNA on *hnRNPQ* mRNA expression. Knockdown efficiency was evaluated using one-tenth of the cells used in the IP experiments described in *A*. The expression level of *hnRNPQ* mRNA was normalized to that of *GAPDH*. Data are represented as the mean ± S.D. of $n = 3$ replicate samples. C, immunoblot analyses of FL-A1 and actin (control) in a portion of the lysates used in the IP experiments described in *A*. *D*, RT-qPCR analyses of *IL8* and *GAPDH* (control) mRNA levels in the cells used in the IP experiments described in *A*. The relative mRNA levels in cells treated with si-hnRNPQ compared with those treated with si-NC are shown. Data are represented as the mean ± S.D. of $n = 3$ replicate samples. ***, $p < 0.005$ by Student's *t* test.

The Association between APOBEC1 and IL8 mRNA Is Promoted by hnRNPQ6—As mentioned above, an interaction between APOBEC1 and *IL8* mRNA was not observed in HEK293 cells; therefore, we investigated whether overexpression of hnRNPQ in this cell line could lead to the promotion of this association. As mentioned above, of the seven hnRNPQ isoforms (hnRNPQ1–7), two (hnRNPQ2 and hnRNPQ4) were isolated in the yeast two-hybrid screen (Table 1). Initially, the effects of overexpression of FLAG-tagged hnRNPQ1 (the canonical form), FLAG-tagged hnRNPQ2, or FLAG-tagged hnRNPQ4 on the interaction between Myc-tagged APOBEC1 (Myc-A1) and *IL8* mRNA in HEK293 cells were examined. However, overexpression of these hnRNPQ isoforms did not facilitate this association (data not shown). Similarly, overexpression of FLAG-tagged hnRNPQ3 or FLAG-tagged hnRNPQ7 did not promote an interaction between APOBEC1 and *IL8* mRNA (data not shown). However, overexpression of FLAG-tagged hnRNPQ6 (FL-Q6) led to an association between ectopically expressed Myc-A1 and *IL8* mRNA in HEK293 cells (Fig. 6*A*). Overexpression of FL-Q6 did not affect Myc-A1 pro-

tein expression (Fig. 6*B*) but did enhance *IL8* mRNA expression (Fig. 6*C*). As mentioned above, TNFα-mediated up-regulation of *IL8* expression did not affect co-IP of Myc-A1 and *IL8* mRNA from HEK293 extracts; therefore, elevated *IL8* expression alone could not explain the FL-Q6-mediated association of Myc-A1 with *IL8* mRNA in this cell line. Instead, overexpression of FL-Q6 in HEK293 cells may have promoted or stabilized the association between Myc-A1 and *IL8* mRNA, thereby increasing the stability of the *IL8* mRNA. In support of this theory, siRNA-mediated knockdown of hnRNPQ in HuH7.5 cells attenuated the Myc-A1-dependent increase in the activity of the pLuc-IL8 plasmid, which contained the full-length *IL8* 3′-UTR downstream of a luciferase coding sequence, and overexpression of exogenous FL-Q6 in the hnRNPQ-specific siRNA-treated cells recovered this defect (Fig. 6*D*). These results indicate that hnRNPQ was required for the FL-A1-dependent increase in *IL8* mRNA expression and that hnRNPQ6 led APOBEC1 to stabilize the *IL8* mRNA by binding to its 3′-UTR.

A protein-protein co-IP experiment demonstrated an association between Myc-A1 and FL-Q6 in HEK293 cells (Fig. 6, *E*

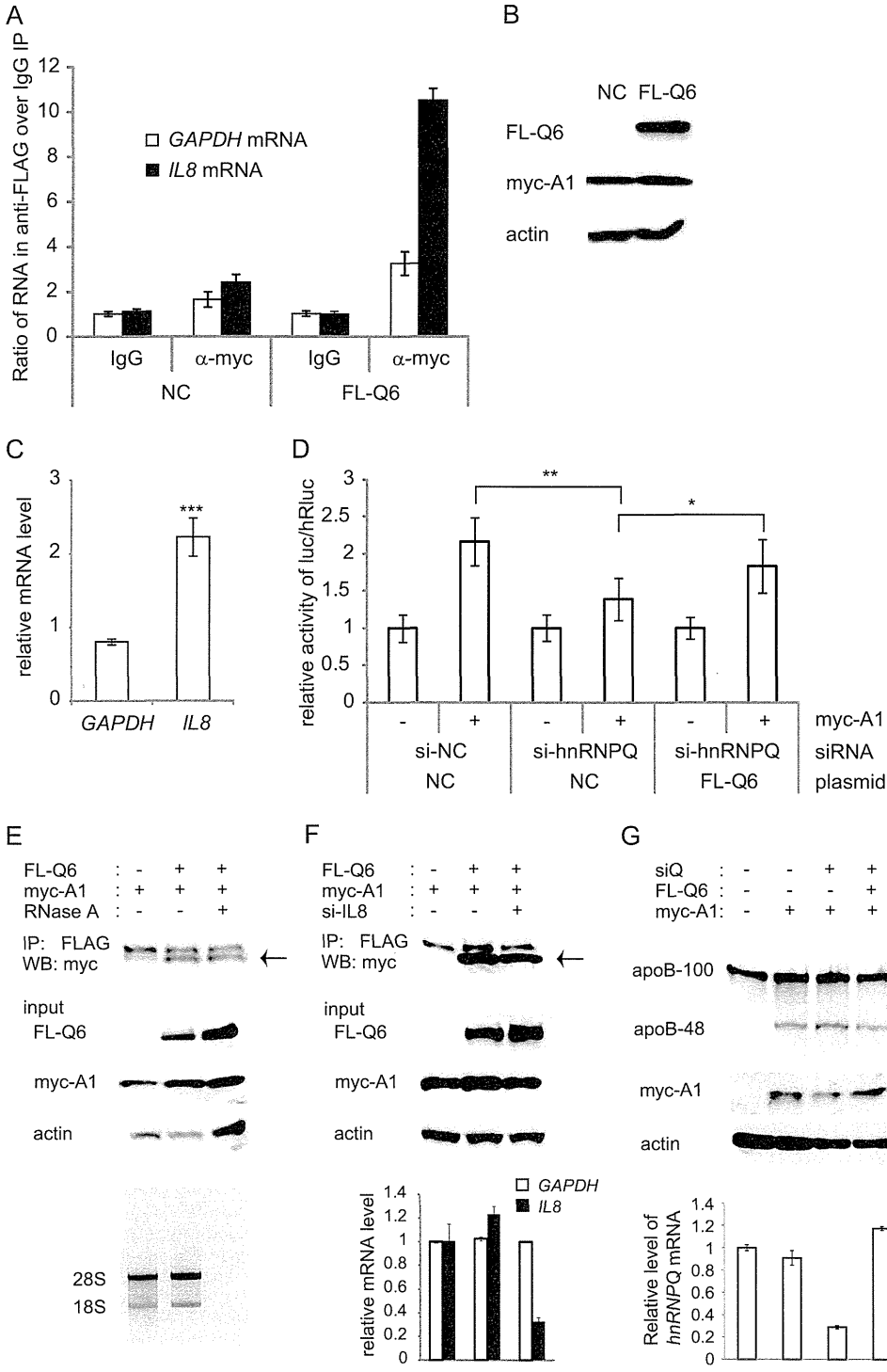

and *F*). This association was not disrupted by RNase treatment (Fig. 6*E*). Moreover, *IL8* mRNA depletion by IL8-specific siRNA did not affect their association (Fig. 6*F*), suggesting that the association between APOBEC1 and hnRNPQ6 was independent of *IL8* mRNA. Taken together, these findings are consistent with the hypothesis that the association between APOBEC1 and hnRNPQ6 promotes binding of APOBEC1 to *IL8* mRNA.

As mentioned above, transient expression of APOBEC1 led to the production of apoB-48 in HuH7.5 cells (Fig. 2*B*). Neither knockdown nor knockdown and subsequent rescue of hnRNPQ6 affected APOBEC1-mediated apoB-48 production in HuH7.5 cells (Fig. 6*G*), suggesting that hnRNPQ6 may not be involved in *APOB* mRNA editing.

Endogenous Expression of hnRNPQ6 Enables APOBEC1 to Increase IL8 Production—The finding that hnRNPQ6 is a complementing protein that facilitates the association between APOBEC1 and *IL8* mRNA led us to examine whether hnRNPQ6 expression levels were positively correlated with the amount of FL-A1/*IL8* mRNA in co-immunoprecipitates prepared from HuH7.5 and HEK293 cell extracts. Because of their sequence similarities, it is difficult to distinguish between the mRNAs encoding the different hnRNPQ isoforms with a single round of qPCR; therefore, two rounds of PCR were performed. For the first round, primers that would amplify *hnRNPQ3*, *hnRNPQ5*, and *hnRNPQ6* (expected sizes: 1584, 1686, and 1686 bp, respectively) were used. A second round of PCR was performed to amplify *hnRNPQ5* and *hnRNPQ6* (expected size: 704 bp) and distinguish these isoforms from *hnRNPQ3*. None of the hnRNPQ isoforms examined were detected in HEK293 cells (Fig. 7*A*). By contrast, cloning and sequence validation of the second-round PCR products from HuH7.5 cells showed that both *hnRNPQ5* and *hnRNPQ6* were expressed in this cell line and that they were expressed at a 1:15 ratio of *hnRNPQ5* to *hnRNPQ6*. These results suggest that hnRNPQ6 is the authentic complementing protein that mediates the association between APOBEC1 and *IL8* mRNA. Moreover, the lower level of association between FL-A1 and *IL8* mRNA observed in HEK293 cells may be due to the lack of hnRNPQ6 in this cell line.

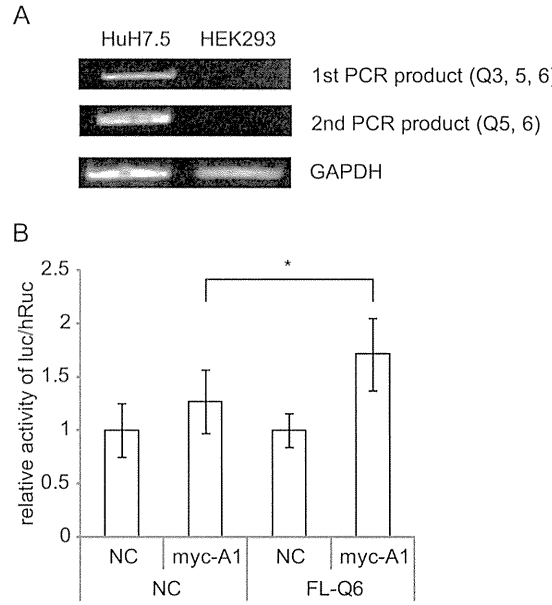

FIGURE 7. **The complementing activity of hnRNPQ6 enables APOBEC1 to regulate IL8 production in HEK293 cells.** *A*, PCR analyses of the expression levels of *hnRNPQ* and *GAPDH* (control) mRNAs in HuH7.5 and HEK293 cells. The first round of PCR was performed using primers designed to amplify *hnRNPQ3*, *hnRNPQ5*, and *hnRNPQ6*; the second round of PCR was performed using primers specific to *hnRNPQ5* and *hnRNPQ6* only. *B*, the effects of overexpression of APOBEC1 (*myc-A1*) and hnRNPQ6 (*FL-Q6*) on the activity of the pLuc-IL8 reporter in HEK293 cells. The cells were reverse-transfected with pLuc-IL8, empty plasmid (pCAG-Myc; *NC*), or a Myc-A1-expressing plasmid and empty plasmid (pcDNA3; *NC*) or an FL-Q6-expressing plasmid. Luciferase activity was examined 48 h after transfection. The activity of the pLuc-IL8 construct was normalized to that of the control pGL4.74[hRluc/TK] construct and the level in the empty plasmid (pCAG-Myc)-transfected cells. Data are represented as the mean ± S.D. of $n = 4$ independent experiments. *, $p < 0.05$ by Student's *t* test.

FIGURE 6. **Overexpression of hnRNPQ6 promotes binding of APOBEC1 to *IL8* mRNA in HEK293 cells.** *A*, the increase in binding of APOBEC1 (*myc-A1*) to *IL8* mRNA following overexpression of FLAG-tagged hnRNPQ6 in HEK293 cells. The cells were co-transfected with the Myc-A1 plasmid and empty plasmid (*NC*) or FL-Q6 plasmid 16 h after seeding and then harvested 48 h after transfection and lysed in RIPA buffer. Each lysate was divided into two fractions, one of which was reacted with control IgG and the other with an anti-Myc antibody. Each immunoprecipitate was subjected to RNA extraction and RT-qPCR. For each mRNA, the amount in the anti-FLAG immunoprecipitate was normalized to that in the IgG immunoprecipitate. Data are represented as the mean ± S.D. (*error bars*) of $n = 3$ replicate samples. *B*, immunoblot analyses of FL-Q6, Myc-A1 and actin (control) in lysates prepared from the cells described in *A*. *C*, RT-qPCR analyses of *IL8* and *GAPDH* (control) mRNA levels in the cells described in *A*. The relative mRNA levels in cells expressing FL-Q6 compared with those in control (*NC*) cells are shown. Data are represented as the mean ± S.D. of $n = 3$ replicate samples. ***, $p < 0.005$ by Student's *t* tests. *D*, the effects of knockdown and rescue of hnRNPQ6 expression on the activity of the pLuc-IL8 reporter plasmid. HuH7.5 cells were reverse-transfected with pLuc-IL8, a Myc-A1-expressing (+) or empty control (−) plasmid, a negative control (si-NC) or hnRNPQ-specific (si-hnRNPQ) siRNA (30 nM), and an FL-Q6-expressing or empty control (*NC*) plasmid. Luciferase activity was examined 48 h after transfection. The activity of the pLuc-IL8 construct was normalized to that of the control pGL4.74[hRluc/TK] construct and the level of the empty plasmid (−)-transfected cells. *, $p < 0.05$; **, $p < 0.01$ by Student's *t* test. Data are represented as the mean ± S.D. of $n = 4$ independent experiments. *E*, IP and subsequent immunoblot analyses (*WB*) of HEK293 cells that were co-transfected with a Myc-A1-expressing plasmid and empty plasmid (pcDNA3-FLAG) or an FL-Q6-expressing plasmid. The cells were seeded 16 h prior to transfection, harvested 48 h after transfection, and then lysed in RIPA buffer. The cell lysates were incubated with or without RNase A (100 μg/ml) at room temperature for 10 min, immunoprecipitated with anti-FLAG antibody, and then probed with an anti-Myc antibody. The *arrow* indicates Myc-A1. A portion of each lysate prepared for IP was used as the input for immunoblot analyses of Myc-A1, FL-Q6, and actin (control) levels. RNA was also extracted from each lysate and separated by agarose gel electrophoresis with ethidium bromide to examine the RNA status by RNase treatment. *F*, the effects of *IL8* mRNA depletion on the association between APOBEC1 and hnRNPQ6. HEK293 cells were reverse-transfected with a control or IL8-specific (*si-IL8*) siRNA (30 nM) and then transfected with empty plasmid (pcDNA3-FLAG) or an FL-Q6-expressing plasmid and Myc-A1-expressing plasmid 16 h later. The cells were harvested 48 h after transfection and lysed in RIPA buffer. The cell lysates were immunoprecipitated with anti-FLAG antibody and then probed with an anti-Myc antibody. The *arrow* indicates Myc-A1. A portion of each lysate prepared for IP was used as the input for immunoblot analyses of Myc-A1, FL-Q6, and actin (control) levels. RNA was also extracted from each lysate to examine the expression level of *IL8* mRNA and *GAPDH* mRNA (control). Data are represented as the mean ± S.D. of $n = 3$ replicate samples. *G*, the effect of knockdown and subsequent rescue of hnRNPQ expression on *APOB* editing by APOBEC1. HuH7.5 cells were reverse-transfected with a control or hnRNPQ-specific (si-Q) siRNA (30 nM) and then co-transfected with the indicated combinations of empty plasmid (pCAG-Myc or pcDNA3-FLAG), FL-Q6-expressing plasmid, or Myc-A1-expressing plasmid 16 h later. The culture medium and cells were harvested 48 h after transfection and used for immunoblot analyses of apoB-100 and apoB-48 (culture medium), and Myc-A1 and actin (cells). RNA was extracted from a portion of the cells and subjected to RT-qPCR analyses of *hnRNPQ* mRNA expression. The *hnRNPQ* mRNA level was normalized to that of *GAPDH*. Data are represented as the mean ± S.D. of $n = 3$ replicate samples.

Overexpression of Myc-A1 alone did not affect the activity of the pLuc-IL8 reporter in HEK293 cells, but co-expression of FL-Q6 and Myc-A1 increased its activity significantly (Fig. 7*B*). Moreover, in HuH7.5 cells, which have much higher expression levels of hnRNPQ6 than HEK293 cells (Fig. 7*A*), knockdown of hnRNPQ attenuated the Myc-A1-mediated up-regulation of pLuc-IL8 activity, and rescue of hnRNPQ6 expression in the knockdown cells restored this defect (Fig. 6*D*).

APOBEC1 Facilitates the Association between hnRNPQ6 and IL8 mRNA—The results described above suggested that an association between hnRNPQ6 and APOBEC1 enables APOBEC1 to up-regulate IL8 production by binding to and stabilizing *IL8* mRNA. To confirm the involvement of hnRNPQ6 in the association between APOBEC1 and *IL8* mRNA further, an anti-FLAG antibody (or IgG as a control) was used to immunoprecipitate FL-Q6 and its associated RNAs from extracts of HEK293 cells overexpressing FL-Q6 alone or FL-Q6 and Myc-A1. The immunoprecipitates were subjected to RNA extraction and subsequent RT-qPCR analyses. In the absence of Myc-A1, the anti-FLAG immunoprecipitates contained slightly more *IL8* mRNA than the IgG immunoprecipitates. By contrast, in the presence of Myc-A1, the amount of *IL8* mRNA in the anti-FLAG immunoprecipitates was 30-fold higher than that in the IgG immunoprecipitates (Fig. 8*A*), suggesting that APOBEC1 enhances the efficiency of the interaction between hnRNPQ6 and *IL8* mRNA. Another possibility is that APOBEC1 serves as a chaperone that stabilizes hnRNPQ6 and is obligatory for its folding and ability to bind to *IL8* mRNA. The expression level of FL-Q6 was unaffected by overexpression of Myc-A1 (Fig. 8*B*). The *IL8* mRNA level was 2.7-fold higher in HEK293 cells that expressed both Myc-A1 and FL-Q6 than in those that expressed FL-Q6 only (Fig. 8*C*); this up-regulation may be due to binding of Myc-A1 to *IL8* mRNA. The results of analyses of the pLuc-IL8 reporter activity in HEK293 cells were concordant with the ability of Myc-A1 to bind to *IL8* mRNA in the presence of FL-Q6 (Fig. 7*B*). Therefore, FL-Q6 may be required for the association between Myc-A1 and *IL8* mRNA in these assays. These findings indicate that hnRNPQ6 may be essential to the APOBEC1/*IL8* mRNA association in some cell types.

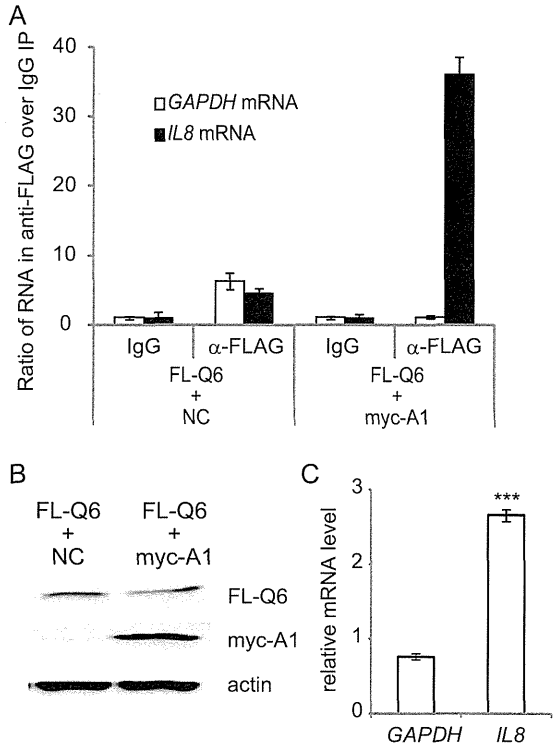

FIGURE 8. **APOBEC1 promotes the interaction of hnRNPQ6 with *IL8* mRNA, and the tripartite association leads to an increase in *IL8* mRNA expression.** *A*, associations between *IL8* mRNA and FL-Q6 in HEK293 cells overexpressing Myc-A1. The cells were seeded 16 h prior to transfection, co-transfected with FL-Q6 and empty plasmid (NC) or a Myc-A1-expressing plasmid, and then harvested 48 h after transfection and lysed in RIPA buffer. Each lysate was divided into two fractions, one of which was reacted with control IgG and the other with an anti-FLAG antibody. Each immunoprecipitate was subjected to RNA extraction and RT-qPCR. For each mRNA, the amount in the anti-FLAG immunoprecipitate was normalized to that in the IgG immunoprecipitate. Data are represented as the mean ± S.D. of $n = 3$ replicate samples. *B*, immunoblot analyses of FL-Q6, Myc-A1, and actin (control) in a portion of the lysates prepared for the IP experiments described in *A*. *C*, RT-qPCR analyses of *IL8* and *GAPDH* (control) mRNA levels in the cells used in the experiment described in *A*. The mRNA levels in the cells expressing both Myc-A1 and FL-Q6 were normalized to those in the cells expressing FL-Q6 only. Data are represented as the mean ± S.D. of $n = 3$ replicate samples. ***, $p < 0.005$ by Student's *t* test.

DISCUSSION

Here, APOBEC1 was associated preferentially with *IL8* mRNA in HuH7.5 cells, and this association was independent of ACF and dependent on hnRNPQ6. Knockdown and overexpression experiments performed in cells demonstrated that APOBEC1 requires hnRNPQ6 to bind to *IL8* mRNA (Figs. 5*A* and 6*A*). There was also a correlation between the APOBEC1/*IL8* mRNA association and *IL8* mRNA level (Figs. 5*D* and 6*C*). The increase in IL8 expression in APOBEC1-expressing HuH7.5 cells was not attributable to transcriptional up-regulation of *IL8* mRNA (data not shown); rather, this increase probably resulted from an extended life span of the *IL8* mRNA caused by binding of APOBEC1/hnRNPQ6. Furthermore, the increased IL8 expression was independent of APOBEC1-mediated RNA editing but required a cluster of AREs in the 3′-UTR of the *IL8* mRNA. Therefore, association with hnRNPQ6/APOBEC1 might affect ARE-mediated decay of *IL8* mRNA. The extended *IL8* mRNA half-life may have allowed for augmented translational elongation or may have increased translational efficiency of *IL8* via an unknown mechanism.

More than 90% of the top 68 RNAs identified in the microarray analysis were mRNAs with at least one AUUUA (ARE) element in their 3′-UTR, indicating that APOBEC1 can bind to various mRNAs that harbor an ARE in this region. In addition, one noncoding RNA (LOC100289230) and two processed pseudogene transcripts (RP11-424A16.1 and AL354718.10) were identified as APOBEC1 binding partners (supplemental Table S1); therefore, APOBEC1 might bind to other types of RNAs in addition to mRNAs.

The microarray analyses identified *CXCL1*, *CXCL2*, *CXCL5*, and *CXCL6* as potential binding targets of APOBEC1 (supplemental Table S1). These mRNAs encode members of the CXC chemokine family, which includes IL8. CXCL1, CXCL2, and IL8 are members of the growth-related oncogene family that contributes to immune infiltration and tumor growth. Overexpression of APOBEC1 in HuH7.5 cells increased the *CXCL2*

and *IL8* mRNA levels but did not affect the *CXCL1*, *CXCL5*, or *CXCL6* mRNA levels (Fig. 2*A*) (data not shown). This result suggests that binding of APOBEC1 does not always result in an increase in the expression level of a target mRNA. APOBEC1 edits the 3′-UTRs of mRNAs, suggesting that it introduces or abolishes target sequences for microRNAs to enable the modification of post-transcriptional processes, including translational efficiency (21). Although we did not identify an APOBEC1-dependent editing event at a specific site in the *IL8* mRNA, it would be worthwhile analyzing other APOBEC1-bound RNAs for editing events.

The yeast two-hybrid analysis revealed that both hnRNPQ2 and hnRNPQ4 can associate with APOBEC1 (Table 1). However, interaction with these proteins was not required for binding of APOBEC1 to *IL8* mRNA. Notably, hnRNPQ1 (also known as GRY-RBP or SYNCRIP) (22) and hnRNPQ6 associate with APOBEC1 to regulate APOBEC1-mediated *APOB* mRNA editing and IL8 production, respectively. Therefore, hnRNPQ2, hnRNP4, or both may be involved in other APOBEC1-dependent functions. The other hnRNPQ isoforms have at least one domain required for association with APOBEC1, namely an N-terminal acidic domain (23) or C-terminal domain (24); therefore, any of these isoforms may associate with APOBEC1 to regulate its function.

In the case of *APOB* mRNA editing, APOBEC1 has various binding partners that act as a complementing factor (ACF) or regulator (such as APOBEC1-binding proteins 1 and 2, hnRNPC1, CUGBP2, Bcl2-associated athanogene-4, and hnRNPQ1) (5, 6, 22, 25–28). Under certain conditions, recombinant APOBEC1 binds directly to the synthetic 3′-UTRs of the *IL8* and *MYC* mRNAs (18). However, the level of binding of APOBEC1 to *IL8* in HuH7.5 cells was higher than the level of binding to *MYC*, although *MYC* is expressed at a relatively high level in these cells (Fig. 1, *A* and *B*). This finding may indicate that hnRNPQ6 does not function as a positive complementary factor that promotes the association of APOBEC1 and *MYC* mRNA. Alternatively, an inhibitory factor may inhibit binding of APOBEC1 to *MYC* mRNA even in the presence of hnRNPQ6. HuH7.5, HuH6, HuS, and PH5CH cells express hnRNPQ6 at comparable levels (data not shown). The HuH6, Hus, and PH5CH cell lines have higher *IL8* mRNA levels than HuH7.5 cells (data not shown); however, the level of binding of APOBEC1 to *IL8* mRNA was highest in HuH7.5 cells (supplemental Table S1 and Fig. 1*C*). These observations indicate that other factors may regulate the association between APOBEC1 and *IL8* mRNA in a cell type-dependent manner.

APOBEC1 mRNA expression is evident in several types of human carcinoma, but an mRNA editing event indicative of its expression is not always obvious (8). Therefore, APOBEC1 may promote carcinogenesis through functions other than RNA editing. In particular, APOBEC1-mediated increases in IL8 production may play a role in tumorigenesis and DNA damage-related pathogenesis.

Acknowledgments—We are grateful to C. Rice for the kind gift of the HuH7.5 cells. We thank R. Shiina and H. Yamamoto (National Center for Global Health and Medicine, Chiba, Japan) for technical assistance.

REFERENCES

1. Greeve, J., Altkemper, I., Dieterich, J. H., Greten, H., and Windler, E. (1993) Apolipoprotein B mRNA editing in 12 different mammalian species: hepatic expression is reflected in low concentrations of apoB-containing plasma lipoproteins. *J. Lipid Res.* **34,** 1367–1383
2. Morrison, J. R., Pászty, C., Stevens, M. E., Hughes, S. D., Forte, T., Scott, J., and Rubin, E. M. (1996) Apolipoprotein B RNA editing enzyme-deficient mice are viable despite alterations in lipoprotein metabolism. *Proc. Natl. Acad. Sci. U.S.A.* **93,** 7154–7159
3. Shah, R. R., Knott, T. J., Legros, J. E., Navaratnam, N., Greeve, J. C., and Scott, J. (1991) Sequence requirements for the editing of apolipoprotein B mRNA. *J. Biol. Chem.* **266,** 16301–16304
4. Richardson, N., Navaratnam, N., and Scott, J. (1998) Secondary structure for the apolipoprotein B mRNA editing site: AU-binding Proteins Interact with a Stem Loop. *J. Biol. Chem.* **273,** 31707–31717
5. Mehta, A., Kinter, M. T., Sherman, N. E., and Driscoll, D. M. (2000) Molecular cloning of Apobec-1 complementation factor, a novel RNA-binding protein involved in the editing of apolipoprotein B mRNA. *Mol. Cell. Biol.* **20,** 1846–1854
6. Lellek, H., Kirsten, R., Diehl, I., Apostel, F., Buck, F., and Greeve, J. (2000) Purification and molecular cloning of a novel essential component of the apolipoprotein B mRNA editing enzyme-complex. *J. Biol. Chem.* **275,** 19848–19856
7. Chester, A., Somasekaram, A., Tzimina, M., Jarmuz, A., Gisbourne, J., O'Keefe, R., Scott, J., and Navaratnam, N. (2003) The apolipoprotein B mRNA editing complex performs a multifunctional cycle and suppresses nonsense-mediated decay. *EMBO J.* **22,** 3971–3982
8. Greeve, J., Lellek, H., Apostel, F., Hundoegger, K., Barialai, A., Kirsten, R., Welker, S., and Greten, H. (1999) Absence of APOBEC-1 mediated mRNA editing in human carcinomas. *Oncogene* **18,** 6357–6366
9. Valdmanis, P. N., Roy-Chaudhuri, B., Kim, H. K., Sayles, L. C., Zheng, Y., Chuang, C. H., Caswell, D. R., Chu, K., Zhang, Y., Winslow, M. M., Sweet-Cordero, E. A., and Kay, M. A. (2013) Upregulation of the microRNA cluster at the Dlk1-Dio3 locus in lung adenocarcinoma. *Oncogene* 10.1038/onc.2013.523
10. Kristensen, D. G., Nielsen, J. E., Jørgensen, A., Skakkebæk, N. E., Rajpert-De Meyts, E., and Almstrup, K. (2014) Evidence that active demethylation mechanisms maintain the genome of carcinoma *in situ* cells hypomethylated in the adult testis. *Br. J. Cancer* **110,** 668–678
11. Chen, X.-J., Mou, X.-Q., Zou, Y.-G., Peng, Z.-Y., Yang, J.-X. (2013) Screening of key genes associated with contused rat spinal cord with DNA microarray. *Eur. Rev. Med. Pharmacol. Sci.* **17,** 2949–2955
12. Ashur-Fabian, O., Har-Zahav, A., Shaish, A., Wiener Amram, H., Margalit, O., Weizer-Stern, O., Dominissini, D., Harats, D., Amariglio, N., and Rechavi, G. (2010) *apoB* and *apobec1*, two genes key to lipid metabolism, are transcriptionally regulated by p53. *Cell Cycle* **9,** 3761–3770
13. Yamanaka, S., Balestra, M. E., Ferrell, L. D., Fan, J., Arnold, K. S., Taylor, S., Taylor, J. M., and Innerarity, T. L. (1995) Apolipoprotein B mRNA-editing protein induces hepatocellular carcinoma and dysplasia in transgenic animals. *Proc. Natl. Acad. Sci. U.S.A.* **92,** 8483–8487
14. Yamanaka, S., Poksay, K. S., Arnold, K. S., and Innerarity, T. L. (1997) A novel translational repressor mRNA is edited extensively in livers containing tumors caused by the transgene expression of the apoB mRNA-editing enzyme. *Genes Dev.* **11,** 321–333
15. Cappione, A. J., French, B. L., and Skuse, G. R. (1997) A potential role for NF1 mRNA editing in the pathogenesis of NF1 tumors. *Am. J. Hum. Genet.* **60,** 305–312
16. Anant, S., and Davidson, N. O. (2000) An AU-rich sequence element (UUUN[A/U]U) downstream of the edited C in apolipoprotein B mRNA is a high-affinity binding site for Apobec-1: binding of Apobec-1 to this motif in the 3′ untranslated region of c-Myc increases mRNA stability. *Mol. Cell Biol.* **20,** 1982–1992
17. Guo, J. U., Su, Y., Zhong, C., Ming, G. L., and Song, H. (2011) Hydroxylation of 5-methylcytosine by TET1 promotes active DNA demethylation in the adult brain. *Cell* **145,** 423–434
18. Anant, S., Murmu, N., Houchen, C. W., Mukhopadhyay, D., Riehl, T. E., Young, S. G., Morrison, A. R., Stenson, W. F., and Davidson, N. O. (2004)

Apobec-1 protects intestine from radiation injury through posttranscriptional regulation of cyclooxygenase-2 expression. *Gastroenterology* **127,** 1139–1149
19. Aly, H. H., Watashi, K., Hijikata, M., Kaneko, H., Takada, Y., Egawa, H., Uemoto, S., and Shimotohno, K. (2007) Serum-derived hepatitis C virus infectivity in interferon regulatory factor-7-suppressed human primary hepatocytes. *J. Hepatol.* **46,** 26–36
20. Ravet, K., Reyt, G., Arnaud, N., Krouk, G., Djouani, E. B., Boucherez, J., Briat, J. F., and Gaymard, F. (2011) Iron and ROS control of the Down-STream mRNA decay pathway is essential for plant fitness. *EMBO J.* **31,** 175–186
21. Rosenberg, B. R., Hamilton, C. E., Mwangi, M. M., Dewell, S., and Papavasiliou, F. N. (2011) Transcriptome-wide sequencing reveals numerous APOBEC1 mRNA-editing targets in transcript 3′ UTRs. *Nat. Struct. Mol. Biol.* **18,** 230–236
22. Blanc, V., Navaratnam, N., Henderson, J. O., Anant, S., Kennedy, S., Jarmuz, A., Scott, J., and Davidson, N. O. (2001) Identification of GRY-RBP as an apolipoprotein B RNA-binding protein that interacts with both Apobec-1 and Apobec-1 complementation factor to modulate C to U editing. *J. Biol. Chem.* **276,** 10272–10283
23. Quaresma, A. J. C., Oyama, S., Jr., Barbosa, J. A. R. G., and Kobarg, J. (2006) The acidic domain of hnRNPQ (NSAP1) has structural similarity to Barstar and binds to Apobec1. *Biochem. Biophys. Res. Commun.* **350,** 288–297
24. Lau, P. P., Chang, B. H. J., and Chan, L. (2001) Two-hybrid cloning identifies an RNA-binding protein, GRY-RBP, as a component of apobec-1 editosome. *Biochem. Biophys. Res. Commun.* **282,** 977–983
25. Lau, P. P., Zhu, H.-J., Nakamuta, M., and Chan, L. (1997) Cloning of an Apobec-1-binding protein that also interacts with apolipoprotein B mRNA and evidence for its involvement in RNA editing. *J. Biol. Chem.* **272,** 1452–1455
26. Lau, P. P., Villanueva, H., Kobayashi, K., Nakamuta, M., Chang, B. H.-J., and Chan, L. (2001) A DnaJ protein, Apobec-1-binding protein-2, modulates apolipoprotein B mRNA editing. *J. Biol. Chem.* **276,** 46445–46452
27. Anant, S., Henderson, J. O., Mukhopadhyay, D., Navaratnam, N., Kennedy, S., Min, J., and Davidson, N. O. (2001) Novel role for RNA-binding protein CUGBP2 in mammalian RNA editing: CUGBP2 modulates C to U editing of apolipoprotein b mRNA by interacting with APOBEC-1 and ACF, the APOBEC-1 complementation factor. *J. Biol. Chem.* **276,** 47338–47351
28. Lau, P. P., and Chan, L. (2003) Involvement of a chaperone regulator, Bcl2-associated athanogene-4, in apolipoprotein B mRNA editing. *J. Biol. Chem.* **278,** 52988–52996

PLOS | ONE

Critical Role of Interferon-α Constitutively Produced in Human Hepatocytes in Response to RNA Virus Infection

Yoji Tsugawa[1,2], Hiroki Kato[3], Takashi Fujita[3], Kunitada Shimotohno[4], Makoto Hijikata[1,2]*

1 Laboratory of Human Tumor Viruses, Institute for Virus Research, Kyoto University, Kyoto, Japan, **2** Laboratory of Viral Oncology, Graduate School of Biostudies, Kyoto University, Kyoto, Japan, **3** Laboratory of Molecular Genetics, Institute for Virus Research, Kyoto University, Kyoto, Japan, **4** The Research Center for Hepatitis and Immunology, National Center for Global Health and Medicine, Ichikawa, Japan

Abstract

Several viruses are known to infect human liver and cause the hepatitis, but the interferon (IFN) response, a first-line defense against viral infection, of virus-infected hepatocytes is not clearly defined yet. We investigated innate immune system against RNA viral infection in immortalized human hepatocytes (HuS-E/2 cells), as the cells showed similar early innate immune responses to primary human hepatocytes (PHH). The low-level constitutive expression of IFN-α1 gene, but not IFN-β and IFN-λ, was observed in both PHH and HuS-E/2 cells in the absence of viral infection, suggesting a particular subtype(s) of IFN-α is constitutively produced in human hepatocytes. To examine the functional role of such IFN-α in the antiviral response, the expression profiles of innate immune-related genes were studied in the cells with the treatment of neutralization against type I IFN receptor 2 (IFNAR2) or IFN-α itself to inhibit the constitutive IFN-α signaling before and after virus infection. As the results, a clear reduction of basal level expression of IFN-inducible genes was observed in uninfected cells. When the effect of the inhibition on the cells infected with hepatitis C virus (HCV) was examined, the significant decrease of IFN stimulated gene expression and the enhancement of initial HCV replication were observed, suggesting that the steady-state production of IFN-α plays a role in amplification of antiviral responses to control the spread of RNA viral infection in human hepatocytes.

Citation: Tsugawa Y, Kato H, Fujita T, Shimotohno K, Hijikata M (2014) Critical Role of Interferon-α Constitutively Produced in Human Hepatocytes in Response to RNA Virus Infection. PLoS ONE 9(2): e89869. doi:10.1371/journal.pone.0089869

Editor: Hak Hotta, Kobe University, Japan

Received September 25, 2013; **Accepted** January 24, 2014; **Published** February 26, 2014

Funding: This work was supported by grants-in-aid from the Ministry of Health, Labour and Welfare of Japan. The funders had no role in study design, data collection and analysis, decision to publish, or preparation of the manuscript.

Competing Interests: The authors have declared that no competing interests exist.

* E-mail: mhijikat@virus.kyoto-u.ac.jp

Introduction

It has been shown that the replication of RNA viruses, including Sendai virus (SeV), Vesicular stomatitis virus, Newcastle disease virus, Sindbis virus, and Hepatitis C virus (HCV) is suppressed by type I interferon (IFN) (IFN-α and IFN-β) produced rapidly from the cells after infection of viruses [1,2]. The cytosolic RNA helicases, including retinoic acid-inducible gene (RIG)-I, have been identified as receptors of pathogen-associated molecular patterns of RNA viruses [3]. After recognition of RNA virus infection by those receptors, signal cascades for induction of IFNs are stimulated and result in the activation of IFN regulatory factor (IRF)-3, and IRF-7 which are transcription factors for induction of type I IFN genes [3,4]. IRF-3 is constitutively produced in many cell types and tissues and phosphorylated after virus infection. Phosphorylated IRF-3 forms a dimer (either a homodimer or a heterodimer with IRF-7) and is translocated to the nucleus. Unlike IRF-3, IRF-7 is constitutively produced only in small amounts, if any, but the gene expression is strongly induced by type I IFN-mediated signaling in most cell types and tissues. The produced IFNs by the way described above then are secreted from the viral infected cells and bind to their receptors, which consist of IFN α/β receptor (IFNAR1 and 2), on the surface of IFN producing and/or neighboring cells and deliver the IFN signal to those cells. The primary role of type I IFN is to limit spread of a variety of pathogens via initiation of the innate immune responses through induction of the genes encoding cytokines and antiviral proteins during the first days of infection [5]. These proteins exhibit antiviral effects both directly by inhibiting viral replication and indirectly by stimulating the adaptive immune system.

On the other hand, constitutive production of type I IFN has been detected in several cells without pathogen stimulation albeit at low level. The constitutive IFN-β has been revealed to be important in maintaining immune homeostasis and essential for immune cell priming [6]. In addition, type I IFN is also known to correlate with multiple biological activities, including anti-proliferative, anti-tumor, pro-apoptotic, and immunomodulatory functions [6,7]. Previously it was reported that the IFN-α mRNA was expressed in the human normal liver [8]. However, what cell type in the human liver is responsible for the expression and what is the biological role have not been clear yet.

Our previous data showed that immortalized human hepatocytes, HuS-E/2 cells, support the whole life cycle of blood-borne HCV (HCVbb) [9]. The infection and proliferation of HCVbb in HuS-E/2 cells were enhanced by ectopic expression of a dominant-negative form of IRF-7, but not that of IRF-3, suggesting that IRF-7, rather than IRF-3, plays a primary role in regulation of HCV proliferation in these cells [10]. IRF-7 mRNA was detected in primary hepatocytes (PHH) and HuS-E/2 cells, but not HuH-7 cells, one of hepatocellular carcinoma derived cell lines, without virus infection [10]. However, the role of

the preexisting IRF-7 and molecular mechanism of its constitutive expression in hepatocytes remains unclear, because of limited knowledge of immediate innate immune response in human hepatocytes.

As the result of study on innate immunity of human hepatocytes, here we report that active IFN-α release occurs in human hepatocytes even in the absence of virus infection. We additionally show that the constitutive IFN-α plays a critical role in the early induction of IFN genes and some IFN stimulated genes (ISGs) through the increase in expression of genes related with induction of such genes, including IRF-7 gene, before virus infection.

Materials and Methods

Cell Culture

HuH-7, Huh-7.5, HepG2, and 293FT cells were grown in Dulbecco's modified Eagle's medium (Nacalai Tesque, Kyoto, Japan) supplemented with 10% fetal bovine serum, 100 U/ml nonessential amino acids (Nacalai Tesque, Kyoto, Japan), and Antimycotic Mixed Stock Solution Penicillin 100 units/ml, Streptomycin 100 μg/ml, Amphotericin B 0.25 μg/ml (Nacalai Tesque, Kyoto, Japan). HuS-E/2 cells were cultured as previously described [10]. PHH were purchased from Gibco (Grand Island, NY, USA), the hepatocyte donor was a 58-year-old male who did not show any evidences of liver abnormalities. PHH were cultured

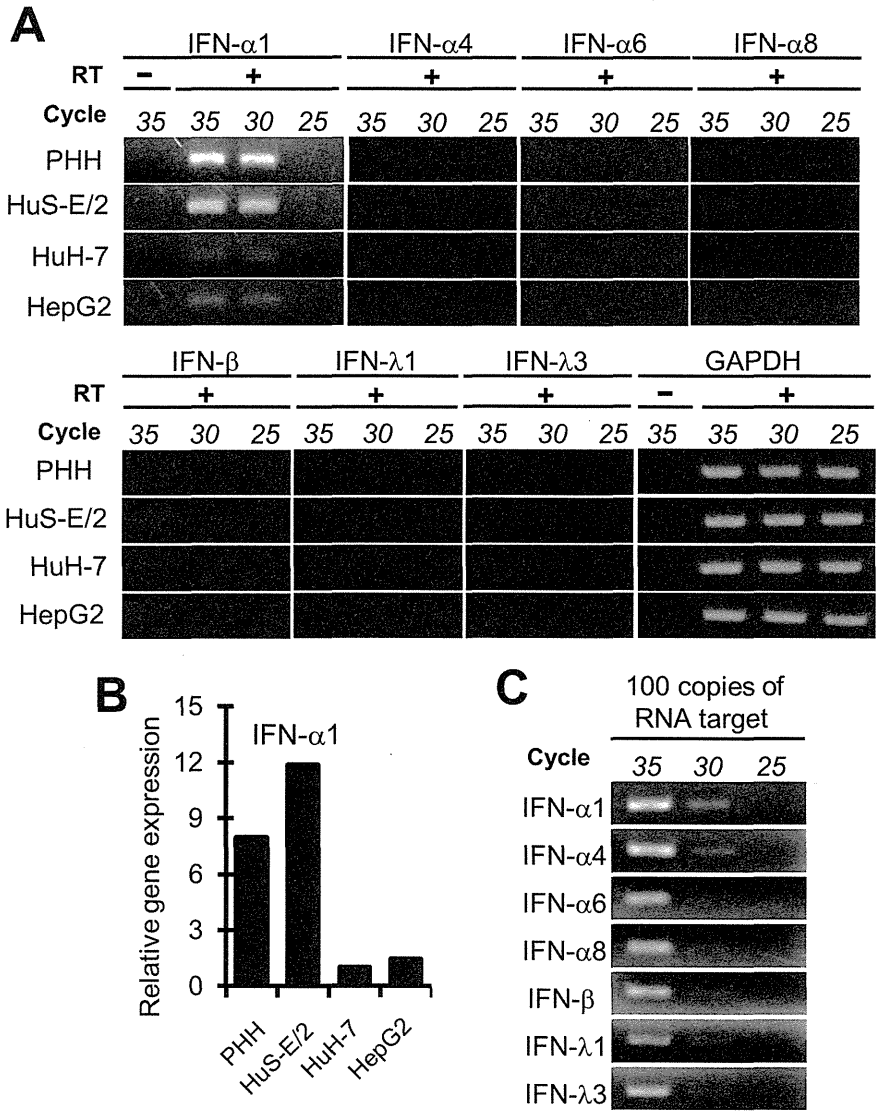

Figure 1. The expression of IFN-α1 gene in the cells derived from human hepatocytes. *A,* The expressions of several IFN genes in human hepatocyte derived cells. The presence of mRNAs for several IFN genes, IFN-α1, IFN-α4, IFN-α6, IFN-α8, IFN-β, IFN-λ1, and IFN-λ3, in PHH, HuS-E/2, HuH-7, and HepG2 cells without virus infection was examined by RT-PCR with different amplification cycles, 25, 30 and 35 cycles. RT-PCR was done with (+) or without (−) reverse transcriptase (RT) reaction. PCR products were separated in the agarose gel and stained with ethidium bromide. GAPDH mRNA was used as an internal standard substance. *B,* Semi-quantitative estimation of IFN-α1 mRNA in those cells. The relative amount of mRNA for IFN-α1 in those cells was estimated by qRT-PCR. The results of qRT-PCR were presented as relative gene expression using the RNA level of HuH-7 cells as a benchmark. *C.* Evaluation of sensitivity of RT-PCR system employed in the detection of IFN subtypes in small quantity. To show the sensitivity of RT-PCR system in this study, RT-PCR was performed with different amplification cycles, 25, 30 and 35 cycles using a primer set described in Table S1 and one hundred copies of in vitro synthesized RNA of each IFN subtype as a template.
doi:10.1371/journal.pone.0089869.g001

in serum-free hepatocyte maintenance medium (Gibco, NY, USA) for one week before starting each experiment.

Treatment with Neutralizing Antibodies (nAb) and Recombinant IFN

Two days prior to stimulation or infection, HuS-E/2 cells were seeded on the collagen coated 12 well plate (8×10^4 cells/well) to yield a confluent cell layer within 24 h. In the case of infection experiment, the cells were treated with nAb mentioned below for 12 hours (hrs). Then the cultured medium contained nAb were replaced with new culture medium containing Sendai virus (SeV) or cell culture derived recombinant HCV (HCVcc) after wash with phosphate buffer saline (PBS). SeV was prepared as described previously [10]. HCVcc was prepared from the HuH-7 or Huh-7.5 cells transfected with in vitro synthesized Jikei Fulminant Hepatitis (JFH) 1^{E2FL} RNA as described previously [11]. Recombinant human IFN-α was obtained from Merck (Darmstadt, Germany). Blocking Antibodies targeting IFN-α (MMHA-2), IFN-β (Rabbit polyclonal antibody), and IFNAR2 (MMHAR-2) were purchased from PBL Biomedical Laboratories (Piscataway, NJ).

RNA Extraction, Reverse-transcriptase Polymerase Chain Reaction (RT-PCR), and Quantitative RT-PCR (qRT-PCR)

Total RNA was isolated from cell cultures with Qiagen RNeasy Mini Kit (Qiagen GmbH, Hilden, Germany). Using 200 ng of total RNA as a template, RT-PCR was done with one-step RNA PCR kit (Takara, Kyoto, Japan) according to the manufacturer's instruction. qRT-PCR was performed with One Step SYBR PrimeScript PLUS RT-PCR Kit (Takara, Kyoto, Japan) by using 7500 Real-time PCR system (Applied Biosystems, Carlsbad CA) according to the manufacturer's instruction. The primer sets used in those PCRs are detailed in Table S1. Real-time PCR data are given as the mean of triplicate samples with standard deviation. The value obtained for the untreated control sample was generally set to 1.

Primer Design and Selection

The primers were designed based on the conserved specific sequence of IFN genes, using primer design software Primer-BLAST (National Center for Biotechnology Information. USA).

To evaluate the sensitivity and specificity of designed primer sets, RT-PCR using those primer sets and in vitro synthesized RNAs for subtypes of IFN as templates was performed. To make the in vitro expression plasmids for the IFNs, the cDNA fragment of each subtype of IFN was synthesized from total RNA from IFN-α stimulated HuS-E/2 cells by RT-PCR and subcloned in to the multiclonning sites of pcDNA3. The RNA fragment of each IFN subtype was synthesized with the plasmid in vitro using the MEGAscript T7 kit (Ambion, Austin, TX) according to the manufacturer's protocol. Synthesized RNA was treated with DNase I followed by acid phenol extraction to remove any remaining template DNA and used for RT-PCR by using one-step RNA PCR kit (Takara, Kyoto, Japan). The amplification conditions were 2 min preheating at 94°C, followed by from 25 to 35 cycles of 10 sec denaturation at 94°C, 30 sec annealing at 55°C, and 1 min elongation at 72°C.

Quantification of Type I IFN

Quantification of active type I IFN was performed by HEK-Blue IFN-α/β cells (Invivogen, San Diego, CA) according to the manufacturer's instruction. Type I IFN concentration (U/ml) was extrapolated from the linear range of a standard curve generated using known amounts of recombinant IFN-α (Merck Darmstadt, Germany).

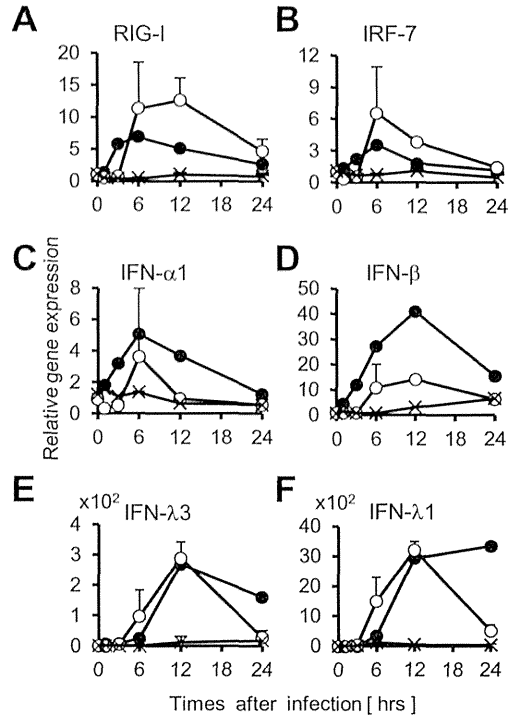

Figure 2. Expression profiles of genes associated with IFN signals in the cells after infection of SeV. Total RNAs were purified from PHH (closed circles), HuS-E/2 cells (open circles), and HuH-7 cells (cross marks) at indicated time points after infection of SeV. Relative quantities of RIG-I (*A*), IRF-7 (*B*), IFN-α1 (*C*), IFN-β (*D*), IFN-λ3 (*E*), and IFN-λ1 (*F*) mRNAs in each total RNA sample were examined by qRT-PCR and plotted using the RNA level firstly detected as a benchmark. The quantity of each RNA sample was normalized by the amount of GAPDH mRNA as relative gene expression. Error bars represent standard deviation (SD) of the mean of determinations from three experiments.
doi:10.1371/journal.pone.0089869.g002

Immunoblotting

Immunoblotting analysis was performed essentially as described previously [12], with slight modifications. Samples of cell lysates were prepared in lysis buffer (50 mM Tris-HCl (pH 8.0), 0.1% SDS, 0.5% sodium deoxycholate, 150 mM NaCl, 5 mM EDTA, 1 mM Orth vanadate (sigma-aldrich, St.Louis, USA), 10 mM NaF, Protease Inhibitor Cocktail (sigma-aldrich St.Louis, USA)). Antibodies used in this study were polyclonal rabbit antiserum against RIG-I at a 1:1000 dilution, IRF-7 at a 1:1000 dilution, STAT1 at a 1:1000 dilution, or p-STAT1 at a 1:1000 dilution. These antibodies were purchased from Cell Signaling Technology (Beverly, MA, USA). Immune-complexes were detected using Western Lightning reagent (PerkinElmer, Waltham, MA) by LAS-4000 system (Fujifilm, Tokyo, Japan).

ELISA for Human IFN-α Protein

Conditioned medium from culture system of HuS-E/2 cells infected with SeV, was collected at 3 and 12 hrs post-infection. The concentration of IFN-α in the conditioned medium was measured with human IFN-α enzyme-linked immunosorbent assay (ELISA) kit (PBL Biomedical Laboratories).

Indirect Immunofluorescence Analysis

Indirect immunofluorescence (IF) analysis was performed essentially as described previously [11]. The primary antibody was anti-SeV polyclonal antibody (1:200) (MBL International

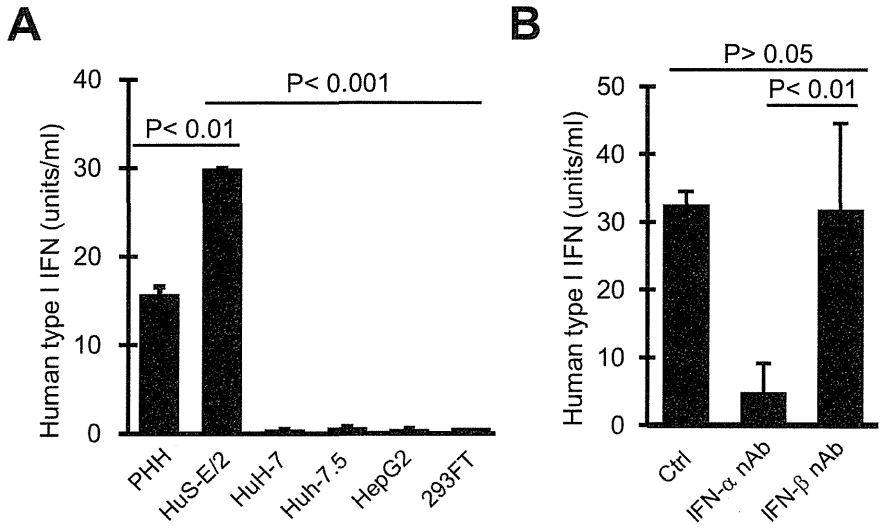

Figure 3. Activity of IFN-α constitutively produced into the culture medium. *A*, Activity of type I IFN produced from the cells without virus infection. Activities of type I IFN produced from PHH, HuS-E/2, HuH-7, Huh-7.5, HepG2, and 293FT cells in the culture media were examined by HEK-Blue™ IFN-α/β cells as described in experimental procedures section and plotted in the graph. *B*, Production of IFN-α from the cells without virus infection. Activity of type I IFN produced from HuS-E/2cells in the culture medium over night was examined as *A*, after treatment with 5 μg/ml neutralizing antibody (nAb) against IFN-α (IFN-α nAb) or IFN-β (IFN-β nAb) for 2 hrs. Error bars represent SD calculated from results of three independent experiments. Probability value (*P* value) was calculated with Student's t test.
doi:10.1371/journal.pone.0089869.g003

Corporation, MA, USA). The fluorescent secondary antibody was Alexa 568-conjugated anti-rabbit (Invitrogen, Carlsbad, CA). Nuclei were stained with 4′,6-diamidino-2-phenylindole (DAPI). The fluorescent signals were visualized by fluorescence microscopy (Bio Zero Keyence Co.).

Results

Induction of IFN Genes and ISGs in PHH and HuS-E/2 Cells by the Infection of Sendai Virus

We examined the antiviral responses of IFN system in some human hepatocyte derived cells against RNA viral infection using sendai virus (SeV) which is a negative strand RNA virus and has been widely used in studies on induction of IFN system [13]. The constitutive expression of IRF-3 and RIG-I genes was commonly found in all those cells as already repoted (data not shown, [10]). Our previous observation that IRF-7 gene was expressed in PHH and HuS-E/2 cells but not in HuH-7 cells under this condition was also confirmed (data not shown, [10]). In addition, the expression of IFN-α1 gene was newly observed in PHH and HuS-E/2 cells albeit at low level (Fig. 1*A*). That, however, was not in the case in HuH-7 and HepG2 cells, although the RT-PCR product was sometimes seen in HuH-7 and HepG2 cells but only vaguely (Fig.1*A*). These results were also confirmed quantitatively by qRT-

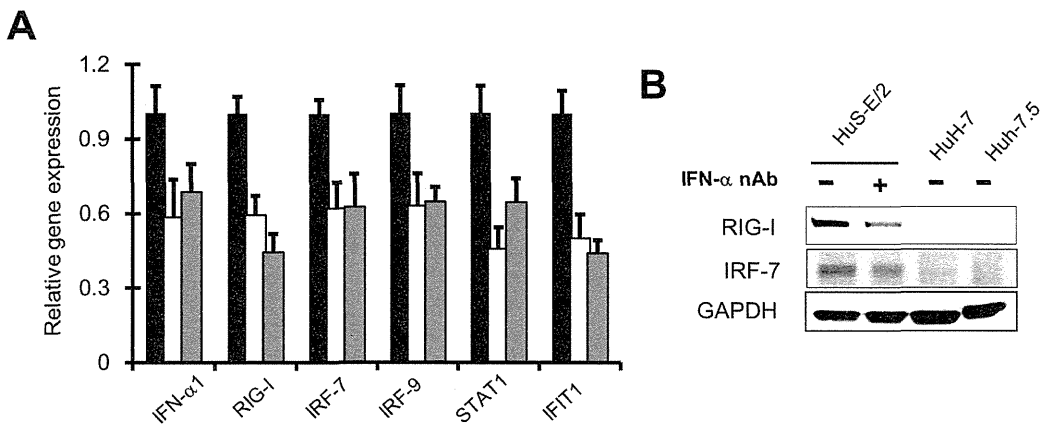

Figure 4. The function of constitutive IFN-α1 on the expression of the genes associated with IFN signals. *A*, The mRNA levels of the genes associated with IFN signals, RIG-I, IRF-7, IRF-9, STAT1, IFIT1, and IFN-α1 itself were examined in HuS-E/2 cells treated with and without nAb against IFN-α (IFN-α nAb, gray bars) (5 μg/ml) or IFNAR2 (IFNAR2 nAb, white bars) (5 μg/ml) for 12 hrs by qRT-PCR. Relative expression level of those genes are plotted using the RNA levels detected in the cells treated without nAb (Mock, black bars) as a benchmark. Results were derived from three independent experiments and error bars represent the calculated SD. *B*, Total cell lysates of HuS-E/2 cells treated with (+) or without (−) 5 μg/ml IFN-α nAb for 12 hrs were analyzed with immunoblotting using antibodies against RIG-I, and IRF-7. Those of HuH-7 and Huh-7.5 cells without treatment were also investigated. Protein levels was normalized among the samples by levels of GAPDH detected with anti-GAPDH antibody.
doi:10.1371/journal.pone.0089869.g004

PCR (Fig. 1*B*). In order to examine the gene expression of the other IFN subtypes in those cells, the primer sets for RT-PCR to detect mRNAs for those factors sensitively and specifically were designed and obtained to use for specific amplification of about one hundred copies of IFN-α4, IFN-α6, IFN-α8, IFN-β, IFN-λ1, or IFN-λ3 mRNAs (Fig. 1*C* and Table S1). Those mRNAs, however, were not detected at all in all cells used in this study by this RT-PCR condition (Fig. 1*A*). These results suggested that IFN-α, at least IFN-α1, but not IFN-β and IFN–λ, is slightly produced in human hepatocytes without virus infection.

Next, the effect of SeV infection on mRNA levels of those genes was investigated in those cells. The mRNA levels of IRF-7 and IFN-α1, a target gene product of IRF-7, were transiently increased and reached peaks 6 hrs post-infection (p.i.) in both PHH and HuS-E/2 cells (Fig. 2*B and 2C*, closed and open circles). Those of IFN-β, and IFN-λ3 reached peaks 12 hrs p.i. in those cells in similar ways (Fig. 2*D and 2E*, open and closed circles). IFN-λ1 mRNA was also increased by 12 hrs p.i. in both HuS-E/2 cells and PHH (Fig. 2*F*, open and closed circles). It decreased from 12 to 24 hrs p.i. in HuS-E/2 cells (Fig. 2*F*, open circles) whereas it slightly increased in PHH (Fig. 2*F*, closed circles). The gene expression of RIG-I, a key factor in the innate immune response to RNA virus infection in many cells [14,15], was also investigated. The increase of RIG-I mRNA was observed from 1 hr to 6 hrs p.i. in PHH (Fig. 2*A*, closed circles). Although that was observed from 3 hrs to 12 hrs p.i., the similar pattern of the increase was observed in HuS-E/2 cells (Fig. 2*A*, open circles). The expressions of RIG-I, IRF-7, and IFNs genes were also assessed in HuH-7 cells following infection. Obvious increase of those mRNAs, however, was not detected in telling contrast to PHH and HuS-E/2 cells (Fig. 2, crosses). These observations indicated that this early innate immune response to SeV infection did not occur in HuH-7 cells. The absence of this early response may explain why HuH-7 cells support efficient proliferation of recombinant HCV [16]. On the other hand, the innate immune response of HuS-E/2 cells against SeV infection seemed to be relatively similar to that of PHH, although the responsiveness curves of those gene expression were slightly different. Thus, we supporsed that HuS-E/2 cells provide a valuable model for studying innate immune response of human hepatocytes against viral infection.

Active IFN-α was Constitutively Produced in HuS-E/2 Cells at a Low Level

In this study, we addressed the constitutive expression of IFN-α1 gene observed in PHH and HuS-E/2 cells, since the detection of IFN-α1 mRNA in the liver tissues from normal human individuals was already detected by RNA blot hybridization, but its function was not cleared yet [8].

The presence of IFN-α in the conditioned medium from HuS-E/2 cell culture system was examined firstly by the ELISA system for IFN-α. However, that was not detected probably because of low concentration of secreted IFN-α and low sensitivity of the system. Then the activity of type I IFN in the culture medium assessed by using HEK-Blue type I IFN assay system in which the cells are designed to produce embryonic alkaline phosphatase protein in type I IFN receptor signaling-dependent manner. As shown in Fig. 3*A*, the culture medium from HuS-E/2 cell culture system showed significantly higher activity of type I IFN than those from the culture systems for Huh-7.5, HuH-7, and HepG2 cells as well as 293FT cells, a cell line derived from human embryonic kidney. To confirm above results further, the effect of neutralizing antibody (nAb) targeting IFN-α on the above conditioned medium was examined similarly. As shown in Fig. 3*B*, the pretreatment of the conditioned medium from HuS-E/2 cell culture with this antibody effectively suppressed the activity of IFN receptor signaling, while nAb targeting IFN-β did not affected (Fig.3*B*). These observations indicated that functional type I IFN was included in the conditioned medium from HuS-E/2 cell culture system and, at least, the majority of the type I IFN in the medium was IFN-α and not IFN-β. From above results, we concluded that HuS-E/2 cells produce functional IFN-α into the culture medium without virus infection.

The Basal Expression of IFN-α1 and ISGs was Elevated by Type I IFN Receptor Signaling

To see whether the IFN-α1 produced in the cells without virus infection affects the cells through the autocrine or paracrine signaling regardless of low level production, the basal expression of several ISGs in HuS-E/2 cells cultured in the medium containing nAb targeting IFNα/β receptor (IFNAR) 2, one of the receptors for type I IFN, were investigated. As shown in Fig. 4*A*, it was clearly observed that the mRNA levels of RIG-I, IRF-7, IRF-9, signal transducer and activator of transcription (STAT) 1, and IFN-induced protein with Tetratricopeptide 1 (IFIT1) were diminished in the cells with the nAb treatment, compared to mock treated cells. Quite similar results were observed in the cells treated with nAb targeting IFN-α (data not shown). The basal expression level of IFN-α1 gene was also reduced by these treatments (Fig. 4*A*). Decreased protein levels of RIG-I and IRF-7 were also observed in HuS-E/2 cells treated with nAb targeting IFN-α, while these proteins were below the detectable level in HuH-7 and Huh-7.5 cells as predicted (Fig. 4*B*). As the treatments of two different nAbs showed the similar results to each other, it was suggested that the type I IFN receptor signaling upregulates the expression of those ISGs, as well as IFN-α1 gene, in basal level in HuS-E/2 cells to some extent.

Basal Production of IFN-α in HuS-E/2 Cells Contributes to Rapid Antiviral Response during Early Phase of Infection

To study the functional role of basal level production of IFN-α in HuS-E/2 cells, the innate immune responses of the cells treated with the above nAbs against the RNA virus infection was investigated. In this experiment, HuS-E/2 cells pretreated with nAbs for 12 hrs to interrupt the basal IFN signaling were exposed to the fresh culture medium contained SeV for 30 min after rinsing the nAbs off from the cells. After the infection, the cells were cultured for 3 hrs and then used as follows (Fig. 5*A*). As the induced expression of RIG-I gene, used as a representative of ISGs, by the treatment with recombinant IFN-α was observed similarly in both cells pretreated with and without nAbs (Fig. 5*B*), it was clearly shown that the cells pretreated with the nAbs retained responsiveness to IFN-α rinsing procedure. At first, the levels of mRNAs for RIG-I, IRF-7, IFN-α1, IFN-β, IFN-λ1, and IFN-λ3 were examined in the cells with or without SeV infection. As shown in Fig. 5*C*, almost the similar patterns of increases of those mRNAs were observed in the cells with SeV infection, although only minor levels of the induction were found in the cases of IRF-7 and IFN-α mRNAs even in the mock pretreated cells. In all the cases, nAb pretreatments effectively suppressed the increases of those mRNAs 3 hrs after SeV infection (Fig. 5*C*). As shown in Fig. 5*D*, the suppression of IFN-α protein production in the culture medium 12 hrs after the infection was also observed by using ELISA.

Next, to examine the effect of the pretreatments with nAbs on virus-induced STAT1 activation, phosphorylated form of STAT1, activated form of STAT1, was detected in SeV infected cells pretreated with nAbs by western blot analysis using anti-

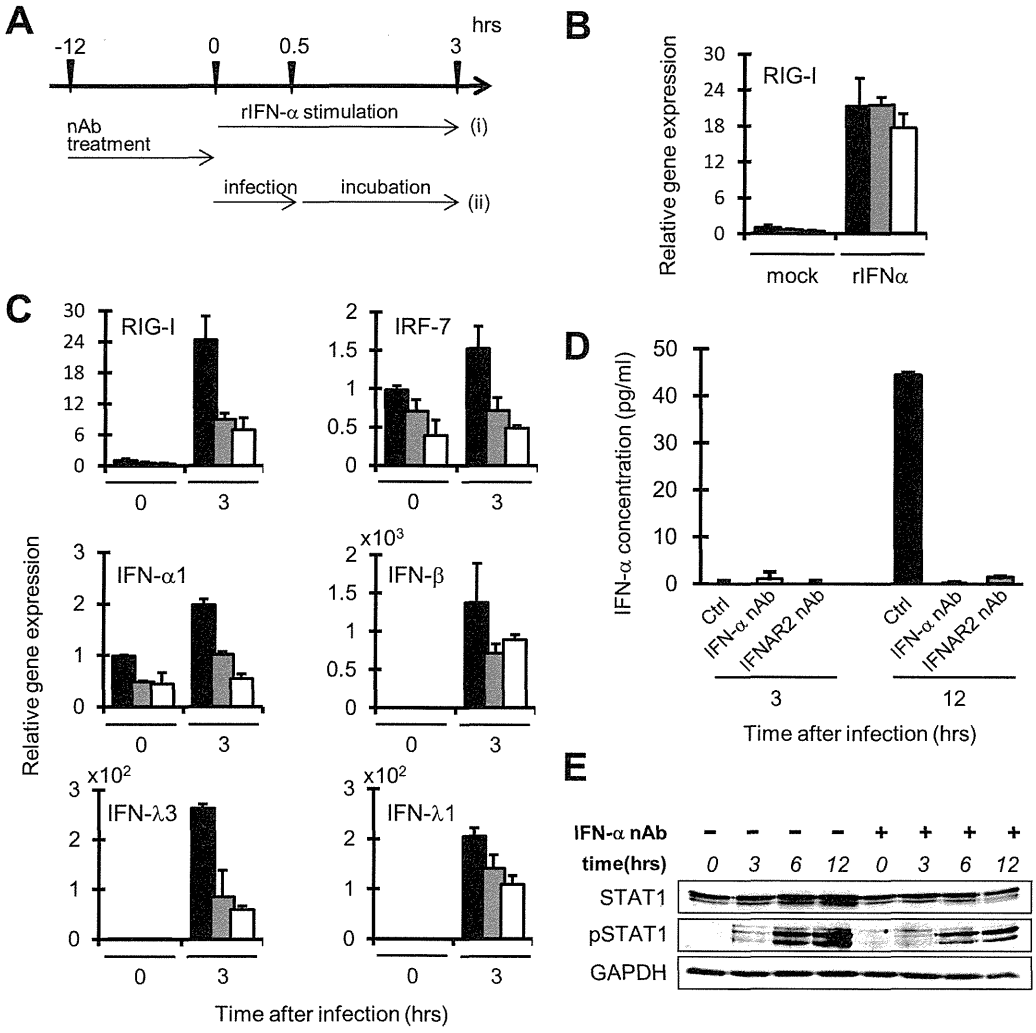

Figure 5. Roles of Constitutive IFN-α on the virus-induced antiviral responses in HuS-E/2 cells. *A*, Schematic of the time schedules for the experiments of recombinant human IFN-α (rIFN-α treatment (i) or SeV infection (ii) after nAb treatment. *B*, Responses of the cells pretreated with IFN-α or IFNAR2 nAbs against exogenous stimulation of rIFN-α. RIG-I mRNA in the cells treated with rIFN-α (2.5 unit/ml) (i) for 0 and 3 hrs after the treatment with IFNAR2 nAb (gray bars), IFN-α nAb (white bars) or mock (black bars) were analyzed by qRT-PCR. Relative expression level of those genes are plotted using each RNA level detected in the cells treated with mock for 0 hr as a benchmark (*B, C*). Error bars represent the calculated SD from the results obtained in three independent experiments (*B, C, D*). *C*, Responses of the cells pretreated with IFN-α or IFNAR2 nAbs against SeV infection. IFN-α1, IFN-β, IFN-λ1, IFN-λ3, and IRF-7 mRNAs in the cells processed as described for panel *B* except infection of SeV (ii) instead of rIFN-α treatment, were analyzed by qRT-PCR. *D*, SeV infection induced IFN-α production from the cells pretreated with IFN-α or IFNAR2 nAbs. Quantity of IFN-α protein in the culture medium was determined by ELISA at 3 and 12 hrs post-infection of SeV. The cells were processed as described for panels *C. E.* STAT1 phosphorylation in the cells pretreated with IFN-α nAbs after SeV infection. The phosphorylation status of STAT1 in the cells processed as described for panel *D* except pretreatment with (+) or without (−) IFN-α nAb only was analyzed by western blot analysis using anti-STAT1 antibody (STAT1), anti-phosphorylated STAT1 antibody (pSTAT1) at 3, 6, and 12 hrs post-infection of SeV. Protein levels were normalized among the samples by levels of GAPDH detected with anti-GAPDH antibody.
doi:10.1371/journal.pone.0089869.g005

phosphorylated STAT1 (pSTAT1). As shown in Fig. 5*E*, the level of pSTAT1 found in the SeV infected cells without IFN-α nAb pretreatment was apparently reduced in the cells with pretreatment at 3, 6 and 12 hrs post-infection, although the protein levels of STAT1 were not affected by the pretreatment, suggesting that pretreatment by IFN-α nAb suppressed the IFN signaling induced by virus infection.

These results suggested that IFN-α produced in the HuS-E/2 cells without virus infection plays a role in the enhancement of initial response of IFN system.

IFN-α Released from HuS-E/2 cells without Viral Infection Contributes to Inhibit Initial Infection and Proliferation of RNA Viruses, Including HCV

To examine whether IFN-α produced in the cells without virus infection actually plays a role in prevention of viral infection, the permissiveness of HuS-E/2 cells, which were pretreated with and without IFNAR2 nAb, against SeV infection was investigated. Compared to the cells without pretreatment of nAb (shown as control panels in Fig. 6*A*), the number of SeV infected cells (shown in red) was increased in the cells with treatment both 6 and 9 hrs after infection in time-dependent manner (Fig. 6*B*). We also assessed

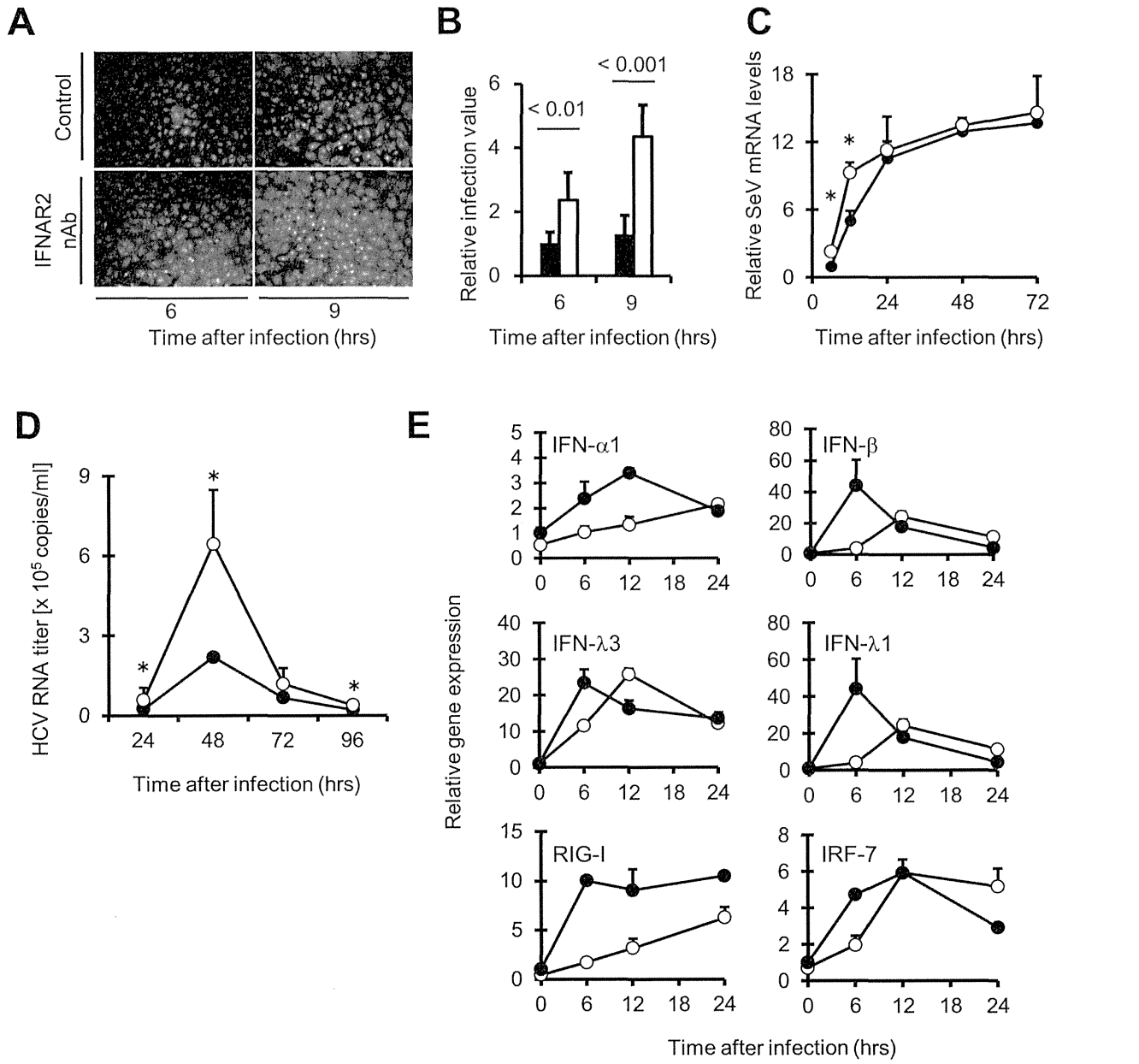

Figure 6. Suppressive role of constitutive IFN-α on viral infection or initial viral proliferation. *A*, Enhanced infection of SeV by neutralization of constitutive IFN-α visualized with IF. Cells were processed basically as described in the figure legend for Fig. 5, panel *C* (*A, B, C, D, E*). At 6 and 9 hrs after SeV infection, the cells were fixed and studied by IF using anti SeV antibodies (red). Nuclei were stained with DAPI (blue). *B*, Numerical conversion of the results in panel *A*. Infection of SeV was quantified by counting of the fluorescent positive cells in ten fields of views per well of two wells. Relative infection values of the cells treated with (white bars) and without (black bars) IFNAR2 nAb were calculated by using the averaged number of infected cells without nAb treatment at 6 hrs postinfection as a benchmark. *P* value was calculated with Student's t test. *C*, Quantification of SeV RNA were measured by qRT-PCR. RNA samples from HuS-E/2 cells pre-treated with (open circles) and without (closed circles) nAb against IFN-α (5 μg/ml) were prepared at the indicated time points (24, 48, and 72 hrs post-infection with SeV). *D*, HCV RNA copies in HuS-E/2 cells pre-treated with (open circles) and without (closed circles) IFN-α nAb at the indicated time points (24, 48, 72, and 96 hrs post-infection with HCVcc) were measured by qRT-PCR. *E*, Time course expression of IFN-α1, IFN-β, IFN-λ1, IFN-λ3, RIG-I and IRF-7 mRNAs in the cells pre-treated with (open circles) or without (closed circles) IFN-α nAb during early stage of HCV infection (6, 12, 18, and 24 hrs post-infection with HCVcc). For each analysis, the results are normalized to the value obtained from the mock treatment. Error bars represent the calculated SD from the results obtained in three independent experiments (*B, C, D, E*).
doi:10.1371/journal.pone.0089869.g006

the proliferation of SeV in HuS-E/2 cells with or without pretreatment of IFN-α nAb by quantitative estimation of SeV genomic RNA. As shown in Fig. 6*C*, the increase of SeV genomic RNA levels was clearly observed in the cells with the pre-treatment at 12 hrs post-infection, suggesting that the preexisting IFN-α play a suppressive role on SeV proliferation during early phase of infection. In addition, to investigate the effect of constitutive IFN-α on the hepatotropic virus, we examined the infection and proliferation of HCVcc in HuS-E/2 cells with or without pretreatment of IFN-α nAb. As shown in Fig. 6*D*, the transient

infection and proliferation of HCVcc was observed in the HuS-E/2 cells as previously reported [10]. It was clearly observed that HCV RNA levels in the cells with the pretreatment were significantly higher than the cells without pretreatment from 24 to 48 hrs post-infection, although the significant difference was not observed in each cells from 72 to 96 hrs post-infection (Fig. 6*D*). Next, the expression of several IFN related genes in HuS-E/2 cells with or without the pretreatment was examined after HCVcc infection. As shown in Fig. 6*E*, compared to the cells without pretreatment, the delayed increases of RNAs for IFN-α1, IFN-β, IFN-λ1, IFN-λ3, RIG-I and IRF-7 after HCV infection were observed in HuS-E/2 cells with the pretreatment, although induction patterns were varied among those genes. These results suggested that IFN-α produced from HuS-E/2 cells without virus infection contributes to rapid antiviral innate immune response of the cells to limit the proliferation of HCV during the initial stage of infection.

Discussion

In this study, we showed that IFN-α1 gene is expressed in HuS-E/2 cells without virus infection as in the case of PHH, albeit at a low level and that the IFN-α, including IFN-α1, functions to elevate the expression of the genes related with anti-viral innate immune system in the cells. Previously, the expression pattern of the genes related with innate immunity of the HuS-E/2 cells, was shown to be similar to that of PHH [10]. The constitutive expression of IFN-α1 gene was also previously observed in human liver tissue [8]. Our results, therefore, suggested that the previous detection of IFN-α1 mRNA in normal human liver is due in part at least to the gene expression in hepatocytes in that tissue. The constitutive production of type I IFN has been reported previously in several tissues mainly concerning IFN-β [17,18,19,20]. The mechanisms that support the constitutive production of IFN-β have been relatively studied well and revealed to be involved with multiple transcription factors, such as c-Jun and RelA [6]. However, molecular mechanism that controls the steady-state production of IFN-α has been largely unclear. The transcriptional promoter region of IFN-α1 gene contains two regulatory elements, one is homologous to the positive regulatory domain I (PRDI) of the IFN-β gene promoter [21,22,23] and another is virus-responsive enhancer module, as proposed to a TG-like domain [24,25]. Our previous report showed that IRF-7 gene is constitutively expressed in HuS-E/2 cells [10]. IRF-7, together with IRF-3, is known to play a pivotal role in the induction of IFN-α and IFN-β genes through binding with PRDI in cells infected with virus [3,4], although it was suggested that IRF-7, rather than IRF-3, is important to suppress the infection and replication of HCV in the cells [10]. The basal expression of IFN-α and IFN-β genes, however, was reported not to depend on these regulatory factors [26]. We also observed that silencing IRF-7 in HuS-E/2 cells with shRNA method did not diminish the steady-state level expression of IFN-α1 (data not shown). We found some sequences homologous to the binding sites for some hepatocyte-specific transcription factors, including hepatocyte nuclear factor 1α (HNF1α), HNF1β, and HNF4α within the region 5000 base pairs upstream of the transcription start site of IFN-α1 gene using computational promoter analysis (data not shown). It, therefore, may be possible that the tissue-specific transcription factor contributes to the expression of IFN-α1 gene in a tissue-specific manner. As a recent study showed that tissue–specific differences in IFN genes or ISG expression can be attributed in part to the epigenetic regulation [27], it is probable that the innate immune phenotypes of IFN-α gene in human hepatocytes is also associated with tissue-specific patterns of histone modification. Further study is needed to clarify the molecular mechanisms of constitutive expression of IFN-α1 gene in human hepatocytes.

The results obtained from this study showed the functional role of the constitutive IFN-α in human hepatocytes on the immediate innate immune response against RNA virus infection, including HCV, through augmentation of the steady-state level expression of several genes related to detection of the infection and induction of IFN systems, such as RIG-I, IRF-7, and IFNs genes. Rapid activation of IFN system should be important to suppress the expansion of viral infection. The constitutive IFN-β has been reported previously in several tissues and was demonstrated to strengthen IFN response toward viral infection [17,18,19,20]. This constitutive IFN-β involves a positive feedback loop as proposed in a "revving-up model" in such tissues [28]. The weak cellular signals constantly introduced by constitutive IFN-β allows cells to elicit a more robust response against viral infection than the cells without such signals [17]. This signaling likely occasion induction of the IRF-7 gene without viral infection as a priming effect [29]. Cardiac myocytes was reported to produce higher basal IRF-7 without viral infection through the Jak-STAT pathway activated with preexisting IFN-β for instant antiviral response [20]. Plasmacytoid dendritic cells (pDCs) are known to produce IFN-α and IRF-7 constitutively just like human hepatocytes reported in this study. pDCs respond rapidly and effectively to a range of viral pathogens with high production of IFN-α in constitutive IRF-7 production dependent manner [30,31,32]. These suggested that IRF7, of which gene expression is induced by constitutive type-I interferon, both IFN-α and IFN-β, in those cells, plays a crucial role in the priming effect on the consecutive and rapid anti-viral innate immune response.

The liver is the largest solid organ in the body with dual inputs for its blood supply. It receives 80% of its blood supply from the gut through the portal vein, which is rich in bacterial products, environment toxins, and food borne pathogens. The remaining 20% of the blood is supplied from vascularization by the hepatic artery [33]. This high exposure to pathogens may require that the liver has an efficient and rapid defensive mechanism against possible frequent infection. Although most pathogens that get at the liver are killed by local innate and adaptive immune responses, hepatitis viruses (such as HBV and HCV) which gain the ingenious function to escape immune control persist in hepatocytes [34,35,36,37,38]. Therefore, further study to reveal the role of steady-state production of IFN-α1 in human hepatocytes may provide new insights into the virus-cell interaction and chronic infection of hepatotropic viruses.

In addition to the importance for the antiviral effect, it has been also proposed that the constitutive IFN-β primes for an efficient subsequent response to other cytokines and are also important for immune homeostasis [39,40,41], maintenance of bone density [42] and antitumor immunity [43]. Further analysis of the possible role of constitutive IFN-α on the other physiological events in human hepatocytes may be required.

Supporting Information

Table S1 List of names and sequences of the primers and expected sizes of RT-PCR products using those primers.
(TIF)

Author Contributions

Conceived and designed the experiments: YT MH. Performed the experiments: YT HK. Analyzed the data: YT MH. Contributed reagents/materials/analysis tools: TF KS MH. Wrote the paper: YT MH.

References

1. Samuel CE (2001) Antiviral actions of interferons. Clin Microbiol Rev 14: 778–809, table of contents.
2. Randall RE, Goodbourn S (2008) Interferons and viruses: an interplay between induction, signalling, antiviral responses and virus countermeasures. J Gen Virol 89: 1–47.
3. Yoneyama M, Fujita T (2010) Recognition of viral nucleic acids in innate immunity. Rev Med Virol 20: 4–22.
4. Matsumiya T, Imaizumi T, Yoshida H, Satoh K (2011) Antiviral signaling through retinoic acid-inducible gene-I-like receptors. Arch Immunol Ther Exp (Warsz) 59: 41–48.
5. Katze MG, He Y, Gale M, Jr. (2002) Viruses and interferon: a fight for supremacy. Nat Rev Immunol 2: 675–687.
6. Gough DJ, Messina NL, Clarke CJ, Johnstone RW, Levy DE (2012) Constitutive type I interferon modulates homeostatic balance through tonic signaling. Immunity 36: 166–174.
7. Pestka S, Krause CD, Walter MR (2004) Interferons, interferon-like cytokines, and their receptors. Immunol Rev 202: 8–32.
8. Tovey MG, Streuli M, Gresser I, Gugenheim J, Blanchard B, et al. (1987) Interferon messenger RNA is produced constitutively in the organs of normal individuals. Proc Natl Acad Sci U S A 84: 5038–5042.
9. Aly HH, Qi Y, Atsuzawa K, Usuda N, Takada Y, et al. (2009) Strain-dependent viral dynamics and virus-cell interactions in a novel in vitro system supporting the life cycle of blood-borne hepatitis C virus. Hepatology 50: 689–696.
10. Aly HH, Watashi K, Hijikata M, Kaneko H, Takada Y, et al. (2007) Serum-derived hepatitis C virus infectivity in interferon regulatory factor-7-suppressed human primary hepatocytes. J Hepatol 46: 26–36.
11. Miyanari Y, Atsuzawa K, Usuda N, Watashi K, Hishiki T, et al. (2007) The lipid droplet is an important organelle for hepatitis C virus production. Nat Cell Biol 9: 1089–1097.
12. Kushima Y, Wakita T, Hijikata M (2009) A disulfide-bonded dimer of the core protein of hepatitis C virus is important for virus-like particle production. J Virol 84: 9118–9127.
13. Maeno K, Yoshii S, Nagata I, Matsumoto T (1966) Growth of Newcastle disease virus in a HVJ carrier culture of HeLa cells. Virology 29: 255–263.
14. Kato H, Takeuchi O, Sato S, Yoneyama M, Yamamoto M, et al. (2006) Differential roles of MDA5 and RIG-I helicases in the recognition of RNA viruses. Nature 441: 101–105.
15. Kato H, Sato S, Yoneyama M, Yamamoto M, Uematsu S, et al. (2005) Cell type-specific involvement of RIG-I in antiviral response. Immunity 23: 19–28.
16. Blight KJ, McKeating JA, Rice CM (2002) Highly permissive cell lines for subgenomic and genomic hepatitis C virus RNA replication. J Virol 76: 13001–13014.
17. Sato M, Suemori H, Hata N, Asagiri M, Ogasawara K, et al. (2000) Distinct and essential roles of transcription factors IRF-3 and IRF-7 in response to viruses for IFN-alpha/beta gene induction. Immunity 13: 539–548.
18. Lienenklaus S, Cornitescu M, Zietara N, Lyszkiewicz M, Gekara N, et al. (2009) Novel reporter mouse reveals constitutive and inflammatory expression of IFN-beta in vivo. J Immunol 183: 3229–3236.
19. Hsu AC, Parsons K, Barr I, Lowther S, Middleton D, et al. (2012) Critical role of constitutive type I interferon response in bronchial epithelial cell to influenza infection. PLoS One 7: e32947.
20. Zurney J, Howard KE, Sherry B (2007) Basal expression levels of IFNAR and Jak-STAT components are determinants of cell-type-specific differences in cardiac antiviral responses. J Virol 81: 13668–13680.
21. Keller AD, Maniatis T (1988) Identification of an inducible factor that binds to a positive regulatory element of the human beta-interferon gene. Proc Natl Acad Sci U S A 85: 3309–3313.
22. Braganca J, Civas A (1998) Type I interferon gene expression: differential expression of IFN-A genes induced by viruses and double-stranded RNA. Biochimie 80: 673–687.
23. Goodbourn S, Maniatis T (1988) Overlapping positive and negative regulatory domains of the human beta-interferon gene. Proc Natl Acad Sci U S A 85: 1447–1451.
24. Genin P, Braganca J, Darracq N, Doly J, Civas A (1995) A novel PRD I and TG binding activity involved in virus-induced transcription of IFN-A genes. Nucleic Acids Res 23: 5055–5063.
25. MacDonald NJ, Kuhl D, Maguire D, Naf D, Gallant P, et al. (1990) Different pathways mediate virus inducibility of the human IFN-alpha 1 and IFN-beta genes. Cell 60: 767–779.
26. Hata N, Sato M, Takaoka A, Asagiri M, Tanaka N, et al. (2001) Constitutive IFN-alpha/beta signal for efficient IFN-alpha/beta gene induction by virus. Biochem Biophys Res Commun 285: 518–525.
27. Fang TC, Schaefer U, Mecklenbrauker I, Stienen A, Dewell S, et al. (2012) Histone H3 lysine 9 di-methylation as an epigenetic signature of the interferon response. J Exp Med 209: 661–669.
28. Levy DE, Marie I, Smith E, Prakash A (2002) Enhancement and diversification of IFN induction by IRF-7-mediated positive feedback. J Interferon Cytokine Res 22: 87–93.
29. Taniguchi T, Takaoka A (2001) A weak signal for strong responses: interferon-alpha/beta revisited. Nat Rev Mol Cell Biol 2: 378–386.
30. Izaguirre A, Barnes BJ, Amrute S, Yeow WS, Megjugorac N, et al. (2003) Comparative analysis of IRF and IFN-alpha expression in human plasmacytoid and monocyte-derived dendritic cells. J Leukoc Biol 74: 1125–1138.
31. Kerkmann M, Rothenfusser S, Hornung V, Towarowski A, Wagner M, et al. (2003) Activation with CpG-A and CpG-B oligonucleotides reveals two distinct regulatory pathways of type I IFN synthesis in human plasmacytoid dendritic cells. J Immunol 170: 4465–4474.
32. Colantonio AD, Epeldegui M, Jesiak M, Jachimowski L, Blom B, et al. (2011) IFN-alpha is constitutively expressed in the human thymus, but not in peripheral lymphoid organs. PLoS One 6: e24252.
33. Zufferey R, Nagy D, Mandel RJ, Naldini L, Trono D (1997) Multiply attenuated lentiviral vector achieves efficient gene delivery in vivo. Nat Biotechnol 15: 871–875.
34. von Hahn T, Yoon JC, Alter H, Rice CM, Rehermann B, et al. (2007) Hepatitis C virus continuously escapes from neutralizing antibody and T-cell responses during chronic infection in vivo. Gastroenterology 132: 667–678.
35. Gale M, Jr., Foy EM (2005) Evasion of intracellular host defence by hepatitis C virus. Nature 436: 939–945.
36. Li XD, Sun L, Seth RB, Pineda G, Chen ZJ (2005) Hepatitis C virus protease NS3/4A cleaves mitochondrial antiviral signaling protein off the mitochondria to evade innate immunity. Proc Natl Acad Sci U S A 102: 17717–17722.
37. Meylan E, Curran J, Hofmann K, Moradpour D, Binder M, et al. (2005) Cardif is an adaptor protein in the RIG-I antiviral pathway and is targeted by hepatitis C virus. Nature 437: 1167–1172.
38. Foy E, Li K, Wang C, Sumpter R, Jr., Ikeda M, et al. (2003) Regulation of interferon regulatory factor-3 by the hepatitis C virus serine protease. Science 300: 1145–1148.
39. Swann JB, Hayakawa Y, Zerafa N, Sheehan KC, Scott B, et al. (2007) Type I IFN contributes to NK cell homeostasis, activation, and antitumor function. J Immunol 178: 7540–7549.
40. Honda K, Sakaguchi S, Nakajima C, Watanabe A, Yanai H, et al. (2003) Selective contribution of IFN-alpha/beta signaling to the maturation of dendritic cells induced by double-stranded RNA or viral infection. Proc Natl Acad Sci U S A 100: 10872–10877.
41. Musso G, Gambino R, Cassader M (2011) Interactions between gut microbiota and host metabolism predisposing to obesity and diabetes. Annu Rev Med 62: 361–380.
42. Takayanagi H, Kim S, Matsuo K, Suzuki H, Suzuki T, et al. (2002) RANKL maintains bone homeostasis through c-Fos-dependent induction of interferon-beta. Nature 416: 744–749.
43. Jablonska J, Leschner S, Westphal K, Lienenklaus S, Weiss S (2010) Neutrophils responsive to endogenous IFN-beta regulate tumor angiogenesis and growth in a mouse tumor model. J Clin Invest 120: 1151–1164.

VIRAL IMMUNOLOGY
Volume 27, Number 6, 2014

Pp. 285–294
DOI: 10.1089/vim.2013.0140

The J6JFH1 Strain of Hepatitis C Virus Infects Human B-Cells with Low Replication Efficacy

Masato Nakai,[1,2] Tsukasa Seya,[1] Misako Matsumoto,[1] Kunitada Shimotohno,[3] Naoya Sakamoto,[2] and Hussein H. Aly[1,*]

Abstract

Hepatitis C virus (HCV) infection is a serious health problem worldwide that can lead to hepatocellular carcinoma or end-stage liver disease. Current treatment with pegylated interferon, ribavirin, and NS3/4A protease inhibitor would lead to a good prognosis in a large population of patients, but there is still no effective vaccine for HCV. HCV robustly infects hepatocytes in the liver. However, extrahepatic manifestations such as mixed cryoglobulinemia, a systemic immune complex-mediated disorder characterized by B-cell proliferation, which may evolve into overt B-cell non-Hodgkin's lymphoma, have been demonstrated. HCV-RNA is often found to be associated with peripheral blood lymphocytes, suggesting a possible interaction with peripheral blood mononuclear cells (PBMCs), especially B-cells with HCV. B-cell HCV infection was a matter of debate for a long time, and the new advance in HCV *in vitro* infectious systems suggest that exosome can transmit HCV genome to support "infection." We aimed to clarify the susceptibility of primary B-cells to HCV infection, and to study its functional effect. In this article, we found that the recombinant HCV J6JFH1 strain could infect human B-cells isolated from the peripheral blood of normal volunteers by the detection of both HCV-negative-strand RNA by reverse transcription polymerase chain reaction, and NS5A protein. We also show the blocking of HCV replication by type I interferon after B-cell HCV infection. Although HCV replication in B-lymphocytes showed lower efficiency, in comparison with hepatocyte line (Huh7) cells, our results clearly demonstrate that human B-lymphocytes without other non-B-cells can actually be infected with HCV, and that this interaction leads to the induction of B-cells' innate immune response, and change the response of these cells to apoptosis.

Introduction

CHRONIC INFECTION BY HEPATITIS C VIRUS (HCV) is the major cause of liver cirrhosis and hepatocellular carcinoma. About 3.1% of the global population is infected with HCV (50). Historically, a combination therapy with pegylated interferon (IFN) and ribavirin was used for patients infected with genotype 1 HCV. NS3/4A protease inhibitors were recently developed in addition to pegylated IFN and ribavirin, and their combinations have been clinically tried for HCV treatment since then. Although >70% of patients with high viral loads of HCV genotype 1b have a sustained viral response by the therapy using simeprevir or telaplevir with pegylated IFN and ribavirin (17,22), the remaining patients fail to eliminate the virus, and drug resistance remains an issue that must be resolved. Recent development of direct-acting antiviral (DAA) drugs (such as daclatasvir, asunaprevir, and sofosbuvir) are a promising therapeutic option beyond IFN in the treatment of HCV patients (6,32).

HCV is a single-stranded, positive-sense RNA virus in the Hepacivirus genus of the Flaviviridae family. Although HCV is known to infect hepatocytes in the liver and induce hepatitis *in vivo*, *in vitro* cultured primary hepatocytes barely support the HCV life cycle: only hepatoma Huh7 cells and its subclones can efficiently maintain the HCV life cycle of a very limited number of HCV strains *in vitro* (53).

Chronic hepatitis patients with HCV sometimes show other extrahepatic complications such as lymphoproliferative diseases (LPD), including cryoglobulinemia and B-cell malignant lymphoma, autoimmune diseases, and dermatitis (1,12,15,16). Epidemiological analysis shows that chronic HCV patients have higher rates of LPDs than non-HCV-infected populations (36,48,52). Several reports suggested that some lymphotropic HCV strains effectively infected human

Departments of [1]Microbiology and Immunology, and [2]Gastroenterology, Hokkaido University Graduate School of Medicine, Kita-ku, Japan.
[3]Research Center for Hepatitis and Immunology, National Center for Global Health and Medicine, Ichikawa, Japan.
*Present affiliation: Department of Virology II, National Institute of Infectious Diseases, Toyama, Tokyo, Japan.

lymphocytes (20,47), leading to the above-mentioned abnormalities. Infection of lymphocytes with HCV has been a matter of debate for a long time. More than one decade ago, several reports described the existence of HCV-RNA in peripheral blood mononucleated cells (PBMCs) (30,40). The detection rate of HCV-RNA in PBMCs was increased if patients were infected with human immunodeficiency virus (HIV) together with HCV (44). This phenomenon indicated that immune-suppressive circumstances and/or HIV antigen might enhance the replication activity of HCV in lymphoid cells (44). Moreover, it was reported that continuous release of HCV by PBMCs was detected in HCV-infected patients, especially in HIV co-infected patients (7). In addition to HCV-HIV co-infected patients, a low level of HCV replication could be detected in peripheral lymphoid cells from HCV mono-infected patients after antiviral treatment (34,45). Moreover, it was reported that HCV persisting at low levels long after therapy-induced resolution of chronic hepatitis C remained infectious (34). This continuous viral presence could present a risk of infection reactivation.

It has been reported that HCV replication was detected in various kinds of lymphoid cells. Many reports describing the existence of HCV in B-lymphocytes and B-cell lymphoma have been published (21,25,51). Among B-lymphocytes, CD27+ memory B-lymphocytes were more resistant to apoptosis than CD27− B-lymphocytes. CD27+ B-lymphocytes were reported as a candidate subset of the HCV reservoir in chronic hepatitis C (CH-C) (38). On the other hand, others claimed that distinguishing RNA association from true HCV replication was problematic, together with multiple artifacts complicated detection and quantitation of the replicative intermediate minus strand RNA (29,31), and also the failure of retroviral (37) and lentiviral (8) pseudoparticles bearing HCV envelope glycoproteins (HCVpp) to infect primary B-cells or B-cell lines. This led to continuous debate about HCV infection into B-lymphocytes, and the riddle remained unsolved.

Using the recent progress in HCV infection systems, we intended to clarify this debate and analyze HCV infection in human lymphocytes and its functional results. Here, albeit in a lower efficiency compared to HCV infection into Huh7 cells, we report that two different strains of recombinant HCV viruses could infect primary human lymphocytes not only by the detection of HCV-RNA positive and negative strands proliferation, but also NS5A protein detection, and the detection of the activity of luciferase reporter encoded by the recombinant HCV-genome. Blocking of HCV entry using anti-CD81 antibody (Ab), and replication by IFN-α or NS3/4A protease inhibitors successfully suppressed HCV infection. We also found that HCV infection into B-lymphocytes led to the initiation of host response including apoptosis resistance.

Materials and Methods

Cells and reagents

Huh7.5.1 cells were kindly provided by Dr. Francis V Chisari (The Scripps Research Institute, La Jolla, CA). Cells were cultured in high-glucose Dulbecco's modified Eagle's medium (DMEM ; Gibco/Invitrogen, Tokyo, Japan) supplemented with 2 mM L-Glutamine, 100 U of penicillin/mL, 100 μg of streptomycin/mL, 1× MEM non-essential amino acid (Gibco/Invitrogen), and 10% fetal bovine serum (FBS).

Human peripheral blood mononuclear cells (PBMCs) were obtained from healthy volunteers by density gradient centrifugation using Ficoll Paque plus (GE-Healthcare, Waukesha, WI). CD19+ blood cells (representative of human primary B-cells) and CD19− cells (non-B-cells) were separated by MACS CD19 Beads (Milteny Biotec, Bergisch Gladbach, Germany). Purity of CD19+ B-cells was >95% after two-cycle separation. The cells were cultured in RPMI1640 (Gibco/Invitrogen) supplemented with 100 U of penicillin/mL, 100 μg of streptomycin/mL, and 10% FBS.

The following reagents were obtained as indicated: anti-CD81 Ab (BD Pharmingen, Franklin Lakes, NJ); PE anti-CD80 Ab, APC anti-CD86 Ab, and PE-labeled anti-CD19 Ab (eBioscience, San Diego, CA); recombinant IFN-α (Peprotech, Oak Park, CA); BILN2601 (Behringer, Willich, Germany); and Viaprobe 7AAD (BD Bioscience) and Annexin-V-Fluos (Roche, Mannheim, Germany).

Virus propagation

pJ6-N2X-JFH1 was kindly provided from Dr. Takaji Wakita (National Institute of Infectious Diseases, Tokyo) (2). pJc1-GLuc2A was gifted from Dr. Brett D. Lindenbach (Yale University, New Haven) (41). *In vitro* RNA transcription, gene transfection into Huh7.5.1 cells, and preparation of J6JFH1 and Jc1/GLuc2A viruses were performed as previously reported (53). Briefly, the HCV cDNA in plasmids were digested by XBaI and transcribed by T7 Megascript Kit (Invitrogen, Carlsbad, CA). RNA transfection into Huh7.5.1 was performed by electroporation using Gene Pulser II (Bio-Rad, Berkeley, CA) at 260 V and 950 Cap. Culture supernatant were collected on days 3, 5, 7, and 9 of postelectroporation, and concentrated with an Amicon Ultra-15 Centrifugal Filter unit (Millipore, Billerica, MA). The titer of HCVcc was checked by the immunofluoresence method using NS5A antibody when Huh7.5.1 was reinfected with these HCVcc.

Virus infection

Primary B-cells and non-B-cells were cultured with the J6JFH1 HCV strain at a multiplicity of infection (MOI) = 1–3 for 3 h, and cells were harvested after four extensive washes in culture medium. On days 1–6, cells were collected, washed with 0.25% trypsin-EDTA/saline, and incubated with 0.25% trypsin-EDTA for 5 min at 37°C. Then, suspended cells were collected as a source of total RNA. In some experiments, B-cells were infected with the Jc1/GLuc2A strain at MOI = 5 for 3 h. Cells were washed five times in 1× phosphate buffered saline (PBS), and cultured until day 6 for determination of viral replication as GLuc activity with BioLux Gaussia luciferase assay kits (41).

RNA purification, RT-PCR, and quantitative PCR

Total RNA was extracted by using Trizol Reagent (Invitrogen) according to the manufacturer's instructions. Using 100–400 ng of total RNA as a template, we performed RT-PCR and real-time RT-PCR as previously described (3,4). Primer sets are shown in Supplementary Table S1 and Table S2 (Supplementary Data are available online at www.liebertpub.com/vim).

Real-time PCR was used for quantification of positive-strand and negative-strand HCV RNA. Total Trizol-extracted

RNA was analyzed by RT-PCR with a modification of the previously described strand-specific rTth RT-PCR method (10,13). RT primers for complementary DNA synthesis of positive and negative strand HCV RNA are shown in Supplementary Table S1. Positive-strand and negative-strand HCV PCR amplifications were performed using Power SYBR Green PCR Master Mix (Applied Biosystems, Warrington, UK) with 200 nM of paired primers (Supplementary Table S1). The PCR conditions were 95°C for 10 min, followed by 40 cycles at 95°C for 15 sec and 60°C for 1 min.

Virus production and releasing assay

Primary human B-cells were infected with J6JFH1 at MOI = 1. Six days postinfection, the supernatant was collected ("releasing samples"), cells were repeatedly frozen and thawed, and the supernatant was collected ("assembly samples"). Viral titers of "releasing samples" and "assembly samples" were determined with Huh7.5.1 cells using J6JFH1 virus (MOI = 0.001 and 0.01) as control. Total RNA was recovered from the cells on days 2, 4, and 6, and determined with HCV-RNA to check reinfectivity.

Indirect immunofluorescence

Indirect immunofluorescence (IF) expression of HCV proteins was detected in the infected cells using rabbit IgG anti-NS5A antibody (Cl-1) (3). Goat anti-rabbit Alexa 594 (Invitrogen) was used as secondary Ab. Fluorescence detection was performed on the Zeiss LSM 510 Meta confocal microscope (Zeiss, Jena, Germany) (13).

Luciferase assay

Primary B-cells were infected with Jc1/Gluc2A by using concentrated Medium or Mock Medium (PBS-electropolated Huh7.5.1 medium). Media were collected on days 0, 2, 4, and 6 postinfection, cleared by centrifugation (16,000 *g* for 5 min), and mixed with 0.25 volume of *Renilla* 5 lysis buffer (Promega, Madison, WI) to kill HCV infectivity. GLuc activity was measured on a Berthold Centro LB 960 luminescent plate reader (Berthold Technologies, Bad Wildbad, Germany) with each 20 μL sample injected with 50 μL BilLux Gaussia Luciferase Assay reagent (New England Biolabs, Ipswich, MA), integrated over 1 sec.

Cell survival assay

Apoptosis assay: Primary B cells were infected with J6JFH1 virus. Cells were collected 48 h after infection, stained by 7AAD Cell Viability assay kit and Annexin V, and analyzed by FACS Calibur (BD) (13).

ATP assay

Primary B-cells were infected with J6JFH1 virus or Mock concentrated medium. Cells were resuspended and cultured at Lumine plate (Berthold Technologies) postinfection. ATP activities were determined 72 h later using CellTiter-Glo® Luminescent Cell Viability Assay (Promega) according to the manufacturer's protocol.

miRNA detection

Total RNA was extracted by using Qiazol Reagent (Invitrogen). These RNA was purificated and reverse transcripted to cDNA by using the miScript II RT Kit. Synthesized cDNA was used to determine the expression levels of miR-122 (24). Total miRNA was prepared by using Qiazol and miScript II RT kit (Invitrogen), and miR-122 expression was determined by using miScript SYBR Green PCR Kit and miScript Primer Assay (Invitrogen) according to the manufacturer's protocol. U6 small nuclear RNA was used as an internal control.

Results

J6JFH1 infects and replicates in primary B-cells

To address HCV infectivity into primary B-cells, PBMC were isolated from the blood of healthy volunteers and were sorted into CD19+ cells (primary B-lymphocytes) and CD19− cells (non-B-cells). Their purities were >95%. These cells were then incubated with the J6JFH1 HCV. Total RNA was collected on days 2, 4, and 6. The Huh7.5.1 strain was used as positive control. Both Huh7.5.1 and primary B-cells, but not non-B-cells, showed an increase in intracellular HCV-RNA titer, albeit primary B-cells showed lower efficiency than Huh7.5.1 (Fig. 1A). We adjusted the HCV-RNA values using GAPDH as an internal control (Fig. 1B). To confirm J6JFH1 replication in primary B-cells using IF, we also measured the expression of HCV-NS5A, which is a nonstructural protein produced only by the virus secondary to replication. Although the expression was far lower than Huh7.5.1 cells, we managed to detect the NS5A expression in J6JFH1 infected primary B-cells (Fig. 1C).

We examined what kinds of HCV-entry receptors human primary B-cells expressed in our setting. Human CD81, SRB1, and NPC1L1 were expressed, but not the tight junction proteins claudin1 and occludin in mRNA levels (Supplementary Fig. S1). We could not detect miR122 in primary B-cells (Supplementary Fig. S2), expression of which makes the cells permissive to HCV (24). Human CD81 is a primary entry receptor for HCV in hepatocytes (42). Blocking human CD81 by its specific Ab resulted in blockage of HCV infection into primary B-cells, as shown by the suppression of HCV-RNA titer (Fig. 2), suggesting that HCVcc particles enter B-cells also using CD81 receptor. HCV-RNA titer was not suppressed by non-specific Ab (data not shown).

We then examined the effect of the different drugs used to suppress HCV replication (recombinant human IFN, and HCV protease inhibitor, BILN2601). Inhibition of HCV-RNA replication was observed when B-cells were treated with rhIFN-α or BILN2601 (Fig. 2) after infection. BILN2601 showed efficient inhibitory effect on replication of HCV RNA in Huh7.5.1 cells (Supplementary Fig. S3). As control studies, we confirmed that the production of HCV RNA was reduced in Huh7.5.1 cells by CD81 Ab, IFN-α, or BLIN2601 (Supplementary Fig. S4). In both Huh 7.5.1 and B-cells, BLIN2601 most effectively block HCV replication. These data reinforce that HCV is actually replicating in primary B-cells, and that activation of innate immunity by IFN treatment or blocking the NS3/4A protease function is a critical factor in blocking HCV replication in primary B-cells. These data suggest that our system can be used for screening the function of different inhibitors on HCV replication in B-cells.

HCV negative-strand RNA detected in human B-cells

To confirm HCV replication in primary B-cells further, we tested for an increase of negative-strand HCV-RNA after